

## Recent advances in the spin Hall effect of light

This content has been downloaded from IOPscience. Please scroll down to see the full text.

2017 Rep. Prog. Phys. 80 066401

(<http://iopscience.iop.org/0034-4885/80/6/066401>)

View [the table of contents for this issue](#), or go to the [journal homepage](#) for more

### Download details:

This content was downloaded by: xhling

IP Address: 202.120.224.18

This content was downloaded on 30/03/2017 at 10:11

Please note that [terms and conditions apply](#).

## Review

# Recent advances in the spin Hall effect of light

Xiaohui Ling<sup>1,2,3,9</sup>, Xinxing Zhou<sup>4,7</sup>, Kun Huang<sup>5</sup>, Yachao Liu<sup>3</sup>,  
Cheng-Wei Qiu<sup>2,6,7,8</sup>, Hailu Luo<sup>3</sup> and Shuangchun Wen<sup>3</sup>

<sup>1</sup> Hunan Provincial Key Laboratory of Intelligent Information Processing and Application, College of Physics and Electronic Engineering, Hengyang Normal University, Hengyang 421002, People's Republic of China

<sup>2</sup> Department of Electrical and Computer Engineering, National University of Singapore, 4 Engineering Drive 3, Singapore 117576, Singapore

<sup>3</sup> Laboratory for Micro-/Nano-Optoelectronic Devices of Ministry of Education, School of Physics and Electronics, Hunan University, Changsha 410082, People's Republic of China

<sup>4</sup> Synergetic Innovation Center for Quantum Effects and Applications, College of Physics and Information Science, Hunan Normal University, Changsha 410081, People's Republic of China

<sup>5</sup> Agency for Science, Technology and Research, Institute of Materials Research and Engineering, 2 Fusionopolis Way, Innovis, #08-03, Singapore 138634, Singapore

<sup>6</sup> SZU-NUS Collaborative Innovation Center for Optoelectronic Science and Technology, Shenzhen University, Shenzhen 518060, People's Republic of China

<sup>7</sup> NUS Suzhou Research Institute (NUSRI), Suzhou Industrial Park, Suzhou 215123, People's Republic of China

<sup>8</sup> NUS Graduate School for Integrative Science and Engineering, National University of Singapore, Singapore 117456, Singapore

E-mail: [eleqc@nus.edu.sg](mailto:eleqc@nus.edu.sg) (C-W Qiu) and [hailuluo@hnu.edu.cn](mailto:hailuluo@hnu.edu.cn) (H Luo)

Received 16 March 2016, revised 22 October 2016

Accepted for publication 13 December 2016

Published 30 March 2017



Corresponding Editor Professor Masud Mansuripur

## Abstract

The spin Hall effect (SHE) of light, as an analogue of the SHE in electronic systems, is a promising candidate for investigating the SHE in semiconductor spintronics/valleytronics, high-energy physics and condensed matter physics, owing to their similar topological nature in the spin-orbit interaction. The SHE of light exhibits unique potential for exploring the physical properties of nanostructures, such as determining the optical thickness, and the material properties of metallic and magnetic thin films and even atomically thin two-dimensional materials. More importantly, it opens a possible pathway for controlling the spin states of photons and developing next-generation photonic spin Hall devices as a fundamental constituent of the emerging spinoptics. In this review, based on the viewpoint of the geometric phase gradient, we give a detailed presentation of the recent advances in the SHE of light and its applications in precision metrology and future spin-based photonics.

Keywords: spin Hall effect of light, spin Hall shift, geometric phase, weak measurements

(Some figures may appear in colour only in the online journal)

<sup>9</sup>These authors contributed equally to this work.

## 1. Introduction

In 1879, Edwin Hall found that when a magnetic field is applied perpendicular to an electrical conductor carrying an electric current, a voltage difference (the Hall voltage) can be observed across the conductor [1]. This phenomenon was subsequently referred to as the Hall effect. The physical origin of the Hall effect is attributed to the Lorentz force experienced by the charge carriers in the electrical conductor. After the original discovery, a series of Hall effects for electrons, for example the anomalous Hall effect [2], the quantum Hall effect [3, 4], the spin Hall effect (SHE) [5–7], the quantum SHE [8, 9], the quantum anomalous Hall effect [10] and the valley Hall effect [11–13], as well as their photonic counterparts [14–16], have also been presented and investigated. They form a very big family of Hall effects. Two recent articles have reviewed research on the spin–orbit interaction and transverse and longitudinal angular momenta of light, which are of great significance for a comprehensive understanding of Hall effects [17, 18]. Due to their contribution to fundamental science and potential industrial applications, they have been the subject of sustained attention for a long time [19–22].

In addition to their electric charge, electrons have another degree of freedom, namely spin, which corresponds to the SHE stemming from the spin–orbit interaction [5–7]. It manifests as spin accumulations (spin-dependent splitting or shift) of spin-up and spin-down electrons on both lateral boundaries of a current-carrying sample without requiring an applied magnetic field. The SHE has promoted the development of spintronics by offering an effective approach for generating, manipulating, and detecting spin-polarized electrons [19–22]. Analogous to the SHE in electronic systems, the SHE of light, also called the photonic SHE, manifests itself as spin-dependent shifts or spin accumulation of photons, where the spin-1 photon and refractive index gradient correspond to the spin-1/2 electron and electric potential gradient, respectively [17, 18, 23–30].

The spin-dependent shift of light beams was initially investigated in total internal reflection and gradient-index materials several decades ago, where it is referred to as the Imbert–Fedorov effect [31, 32] and the optical Magnus effect [33, 34], respectively. It can be calculated in terms of a stationary-phase argument [35], and can be interpreted by introducing the conservation of angular momentum and the spin–orbit interaction between a photon’s spin and its orbital motion [33–37]. In 2004, Bliokh *et al* interpreted the topological photon spin splitting phenomenon in smoothly inhomogeneous isotropic media in terms of the geometric Berry phase, and connected it to the anomalous Hall effect for electrons [23, 24]. Almost at the same time, Onoda *et al* explained this phenomenon based on the geometric Berry phase and conservation of angular momentum, and referred to it as the ‘Hall effect’ of light [25]. In fact, the Imbert–Fedorov effect and the optical Magnus effect can be viewed as examples of the SHE of light. In 2006, Bliokh *et al* presented a complete theoretical treatment to describe the SHE in the refraction/reflection of a paraxial light beam at an optical interface between two different media [26, 27]. The theory was verified by Hosten and Kwiat in 2008

in a remarkable experiment using a quantum weak measurement technology [28]. In fact, the spin Hall transverse shift is very tiny at subwavelength scale due to the weak spin–orbit interaction and it is difficult to observe directly. The weak measurement experiment is an indirect method that allows the subwavelength spin Hall shift to be enhanced and measured using a position-sensitive detector. Actually, the spin Hall shift of light can also be amplified through multiple reflections in a cylinder glass where the beam shifts can be directly discriminated [29, 30]. Giant SHEs with a beam shift of several wavelengths have been observed in some special situations, such as in nonparaxial light fields [38–42], in optical reflection near the Brewster angle [43–46] and in the presence of topological edge states [47].

The underlying physics of the SHE of light is attributed to the spin–orbit interaction, which corresponds to two kinds of geometric phases: the spin redirection Rytov–Vladimirskii–Berry (RVB) phase related to the change of wave vector direction and the Pancharatnam–Berry (PB) phase associated with the manipulation of the polarization of light [48–52]. When a paraxial beam is reflected or refracted at an optical interface, the polarization vector of each angular spectrum component rotates in momentum space ( $k$  space), acquiring different RVB phases [25–28]. The interference of these modified angular spectrum components results in the redistribution of the light intensity which manifests as a spin-dependent spatial shift of the beam centroid in real space (coordinate space). A paraxial light beam passing through an inhomogeneous anisotropic medium, even at normal incidence, acquires a space-variant PB phase in real space [53–57], resulting in a spin Hall shift in momentum space [58–62]. The shift generated by the RVB phase is extremely tiny in general and can be amplified by weak measurement or in multiple reflections. The spin Hall shift in momentum space produced by the PB phase increases during beam propagation, and can be directly detected without using the weak measurement.

In this review, we will adopt the viewpoint of the geometric phase gradient and focus on the most recent advances in the SHE of light induced by both types of geometric phase in different physical systems. The application of the SHE in precision metrology for optical nanostructures will be discussed. The spin Hall shift in optical interfaces is very sensitive to the optical parameters of materials comprising the interface, such as the refractive index and thickness variation; hence, it is possible to use the SHE of light as a sensitive metrology tool to characterize materials at the nanometer scale [63–65]. The SHE in optics may also serve to explore the SHE in semiconductor spintronics/valleytronics, high-energy physics and condensed matter physics. In high-energy physics, observation of the SHE is beyond existing experimental conditions, and in condensed matter physics its observation is very complicated [19–22, 29, 30, 66–69]. However, in classical optics, the SHE is relatively easy to detect experimentally, and the results can be directly extrapolated to those fields. More importantly, because of the subwavelength-scale shift in the SHE of light, it is expected to enable manipulation of light at the nanoscale. Therefore, the SHE of light offers a convenient and robust opportunity for developing photonic spin

Hall devices analogous to the recently developed spintronic devices, and will bring about a new branch of optics–spinoptics [19–22, 29, 30, 58–62, 70, 71].

It is stated that the so-called ‘optical SHE’ observed in a semiconductor micro-cavity deals with the generation of spin currents of neutral exciton–polaritons [72, 73]. Although it also exhibits the polarization-dependent splitting of light, we exclude it from our consideration due to its slightly different mechanism of combining the elastic scattering of exciton–polaritons and a light-induced magnetic field.

## 2. Geometric phase gradient: a unified description of the SHE of light

The mutual influence and interplay between spin angular momentum (SAM) and orbital angular momentum (OAM) produces the optical spin–orbit interaction. SAM is associated with the elliptical polarization of light [17, 18, 74–76]. The polarization helicity  $\sigma$  takes a value of  $-1$  for left-handed or  $+1$  for right-handed circular polarization, where the handedness is defined from the point view of the source. The two circular polarizations represent the two spin states of the photon in the quantum picture. Each right- and left-handed circular polarized photon carries a SAM of  $+\hbar$  and  $-\hbar$ , respectively, where  $\hbar$  is the reduced Planck constant. There are two types of OAM—intrinsic OAM associated with the optical vortices and extrinsic OAM related to the beam propagation trajectory [17, 18, 74–76]. Intrinsic OAM was recognized by Allen *et al* in the case of a light beam with a helical phase factor  $\exp(-il\varphi)$  (e.g. the Laguerre–Gaussian beam), which carries a well-defined OAM of  $l\hbar$  per photon independent of polarization state [17, 18, 74–76]. Here,  $l$  is a topological charge (arbitrary integer or semi-integer) and  $\varphi$  is the azimuthal angle in the beam’s cross section. The extrinsic OAM depends upon the choice of the coordinate origin and the motion of the centroid of the light beam when propagating at a distance from the coordinate origin [17, 18, 74–76]. It is defined as the cross-product between the transverse position of the beam centroid and its linear momentum, which is similar to the mechanical angular momentum of a classical particle.

The spin–orbit interaction of light between SAM and OAM manifests as a geometric Berry phase and results in a series of SHEs in optics. In 1984, Michael Berry showed that cyclic and adiabatic evolution of a quantum state in parameter space results in a geometric phase [48], now widely known as the Berry phase, in addition to its dynamical counterpart. The Berry phase results from the geometrical properties of the parameter space of the Hamiltonian, which has been generalized to non-cyclic and non-adiabatic evolutions [77–79]. Now it has become a fundamental concept in nearly all branches of physics. Inspired by the Berry phase in quantum mechanics, its optical analog, i.e. the spin redirection RVB phase in momentum space and the PB phase in polarization state space, were rediscovered and intensively investigated in 1980s. The RVB phase associated with the evolution of the propagation direction of light, was initially studied by Rytov in 1938 and

Vladimirskii in 1941, and was rediscovered by Chiao and Wu (who were stimulated by Berry’s 1984 work) in 1986 [80]. The PB phase is relative to the polarization manipulation of light, which was first considered by S. Pancharatnam in crystal optics in 1956 with regard to the phase shift of a light beam whose polarization state is made to change [49]. It was revisited by Berry in 1987, and can be regarded as an optical counterpart of the geometric Berry phase in quantum mechanics [81].

The geometric Berry phase in optics can be interpreted in terms of the coupling between SAM and coordinate rotation [17]. It is very convenient to describe the optical geometric phase in interfacial reflection/refraction and inhomogeneous anisotropic media by considering the local coordinate rotation in the global (laboratory) coordinate. For a circularly polarized plane wave (propagating along the  $z$ -direction) carrying SAM  $\sigma\hat{\mathbf{e}}_z$ , its electric-field polarization vector can be written as  $\mathbf{E}^\sigma \propto \hat{\mathbf{e}}_x + i\sigma\hat{\mathbf{e}}_y$  and  $\hat{\mathbf{e}}_a$  ( $a \in \{x, y, z\}$ ) represents the unit vectors in the corresponding directions. After experiencing a two-dimensional (2D) coordinate rotation by an angle  $\varphi$  with respect to the  $z$ -axis, the resulting light field can be expressed as  $\mathbf{E}^{\sigma'} = \mathbf{E}^\sigma \exp(-i\sigma\varphi)$  with the induced geometric phase term  $\Phi_G = -\sigma\varphi$  expressed as the product of the SAM and rotation angle.

Further, when a paraxial light beam partially reflects and refracts at an optical interface, the polarization vectors of the angular spectrum components (plane waves with slightly different wave-vector directions) of the beam undergo different rotations to satisfy the transversality of electromagnetic fields [25–29]. Each angular spectrum component acquires different spin redirection RVB phases, which form a geometric phase gradient manifesting as a spin Hall shift of the beam centroids. In this process, spin–orbit interaction occurs. The SAM in the normal direction changes upon beam reflection/refraction, so that it must be compensated by a transverse spin Hall shift resulting in a nonzero extrinsic OAM owing to the conservation of total angular momentum in the normal direction. From the viewpoint of the geometric phase gradient, the real-space spin Hall shift ( $\Delta\mathbf{r}$ ) of the beam centroids can be explained as originating from the  $k$ -space RVB phase gradient [17, 62], i.e.  $\Delta\mathbf{r} = \nabla\Phi_{\text{RVB}}(\mathbf{k})$  where  $\Phi_{\text{RVB}}(\mathbf{k})$  is the  $\mathbf{k}$ -dependent RVB phase of the light beam. Typically, for a beam reflecting and refracting at an optical interface, the RVB phase can be written as  $\Phi_{\text{RVB}}(k_y) = \sigma k_y \delta$  which is dependent on  $k_y$ . Here  $k_y$  is a transverse wave vector component and  $\delta$  is associated with the optical parameters of the materials comprising the interface. This phase can be derived by taking into account a series of coordinate rotations and the Fresnel coefficients [82]. For a p-polarized light reflecting at a planar air–glass interface, it reads  $\delta \propto (1 + r_s/r_p)\cot\theta_i/k_0$  with  $\theta_i$  being the incident angle [26–28],  $k_0 = 2\pi/\lambda$  the wave number in a vacuum ( $\lambda$  is the operational wavelength) and  $r_{p(s)}$  the reflection coefficients for p(s)-polarization. Then we can evaluate the spin Hall shift as the gradient of  $\Phi_{\text{RVB}}$ :

$$\Delta\mathbf{r}_y = \nabla\Phi_{\text{RVB}}(k_y) = \frac{\partial\Phi_{\text{RVB}}}{\partial k_y}\hat{\mathbf{e}}_y = \sigma\delta\hat{\mathbf{e}}_y. \quad (1)$$

Thus,  $\Delta \mathbf{r}_y$  is a constant with magnitude  $\delta$ , a tiny value restricted by a fraction of  $\lambda$ . The SHE of light can be adjusted by tailoring the optical parameters of the materials that comprise the interface [82]. In turn, it can be used to identify the optical parameters of nanostructures in precision metrology in terms of the predicted relationship [63–65].

We can now generalize the discussion to the PB phase. The PB phase is linked to the polarization manipulation of light. A typical case is that a birefringent wave plate can imprint an additional geometric PB phase to a light beam even in normal incidence, with the only dependence being upon the optical axis orientation of the wave plate [83]. For a circularly polarized incident wave, the transformation process using Jones matrix representation, neglecting the absorption and loss of the wave plate, can be written as

$$\begin{bmatrix} 1 \\ \sigma i \end{bmatrix} \rightarrow \cos \frac{\psi}{2} \begin{bmatrix} 1 \\ \sigma i \end{bmatrix} + i \sin \frac{\psi}{2} \begin{bmatrix} 1 \\ -\sigma i \end{bmatrix} \exp(i2\sigma\alpha), \quad (2)$$

where  $\alpha$  denotes the orientation of the optical axis and  $\psi$  is the phase retardation of the wave plate. This indicates that some of the incident photons ( $\sin^2\psi/2$ ) reverse their handedness and can be imprinted by an additional PB phase  $2\sigma\alpha$ . The remaining unchanged fraction is ( $\cos^2\psi/2$ ). For a half-wave retardation ( $\psi = \pi$ ), the conversion efficiency is 100%.

If the light beam passes through an inhomogeneous birefringent medium with locally varying optical axis orientations and homogeneous retardation, such as sub-wavelength polarization gratings, liquid crystal  $q$ -plates and plasmonic metasurfaces, it will acquire a spatially varying PB phase [53–57]. In this process the conversion of SAM to intrinsic OAM takes place. The coordinate-related inhomogeneous PB phase forms a phase gradient along the medium surface which manifests as a spin Hall momentum offset [60–62]:

$$\Delta \mathbf{k} = \nabla \Phi_{\text{PB}}(x, y) = \frac{\partial \Phi_{\text{PB}}}{\partial x} \hat{\mathbf{e}}_x + \frac{\partial \Phi_{\text{PB}}}{\partial y} \hat{\mathbf{e}}_y. \quad (3)$$

A typical case of the PB phase in a  $q$ -plate, an inhomogeneous anisotropic medium with azimuthally varying optical axis orientation, reads  $\Phi_{\text{PB}}(x, y) = 2\sigma\alpha(x, y)$  [55, 56], where  $\alpha(x, y) = q\varphi + \alpha_0$  denotes the local, coordinate-dependent optical axis orientation of the  $q$ -plate. Here,  $q$  is an integer of a half-integer,  $\varphi$  is the azimuthal angle and  $\alpha_0$  is a constant defining the initial optical axis orientation for  $\varphi = 0$ . The momentum shift  $\Delta \mathbf{k}$  will induce a real-space shift upon beam propagation which reads [62]

$$\Delta \mathbf{r}_k = \frac{\Delta \mathbf{k}}{k_0} z \quad (4)$$

with  $z$  being the propagation distance.

Up to now, based on geometric phase gradients, we have presented a unified description of the SHE of light. The  $k$ -space RVB phase gradient causes a spin Hall shift in real space, whereas the real-space PB phase gradient leads to a spin Hall shift in the  $k$  space.

### 3. SHE of light induced by the RVB phase

#### 3.1. SHE of light at optical interfaces

Plane-wave reflection and refraction at an optical interface is a fundamental optical process which can be described by Snell's law and the Fresnel formula in a geometrical-optics picture [84]. The propagation evolution of a finite-width paraxial beam, which could be taken as a superposition of many plane waves with slightly different propagation directions, upon an interface, does not exactly follow the geometrical-optics prediction. The remarkable derivation indicates two main beam shifts, i.e. the in-plane Goos–Hänchen shift [85, 86] and the out-of-plane Imbert–Fedorov shift [31, 32, 86], with respect to the plane of incidence.

The Goos–Hänchen shift results from the spatial dispersion of reflection and transmission coefficients of a light beam and the interference of constituent angular spectrum components. The Imbert–Fedorov effect was initially investigated in total internal reflection, which can be viewed as an example of the SHE of light because it shares the same physical origin in the spin–orbit interaction with the SHE. The optical Magnus effect observed in smoothly inhomogeneous media, a photonic version of the mechanical Magnus effect, can also be regarded as an instance of the SHE of light [33, 34]. After the pioneering contributions of the Imbert–Fedorov effect and optical Magnus effect [31–37, 86], Bliokh *et al* [23, 24] and Onoda *et al* [25] in 2004 respectively described the transverse beam shifts in terms of the geometric Berry phase and conservation of total angular momentum along the normal direction of the interface between two different media. Bliokh *et al* considered the topological spin splitting effect as a photonic version of the anomalous Hall effect for electrons, while Onoda *et al* called this effect the ‘Hall effect’ of light. A complete theoretical treatment was given by Bliokh *et al* in 2006, who presented exact expressions for describing the transverse shifts [26, 27]. In the framework of classical electrodynamics, the transverse shifts of a Gaussian beam partially reflecting and refracting at a planar optical interface can be calculated. This process is governed by the law of conservation of the normal component of the total angular momentum for light beams. In 2008, Hosten *et al* [28] employed quantum weak measurement technology for the first time to enhance this weak effect and observed the SHE in an air–glass interface (see the schematic picture in figure 1(a)). The experimental results agree with the theoretical prediction of Bliokh *et al*. Meanwhile, Bliokh *et al* have also demonstrated that the spin Hall shift can be accumulated along a smooth helical trajectory in a cylinder glass and directly observed by measuring the precession of the Stokes vector without using weak measurement technology (figure 1(b)) [29, 30].

The SHE of light in many other interfaces, such as anisotropic crystals [87, 88], semiconductors [89, 90], metals [64, 91], metamaterials/metasurfaces [92–96], multi-layered dielectric films [45, 82, 97], 2D material films [63, 98] and photon tunneling structures [99, 100], has also been

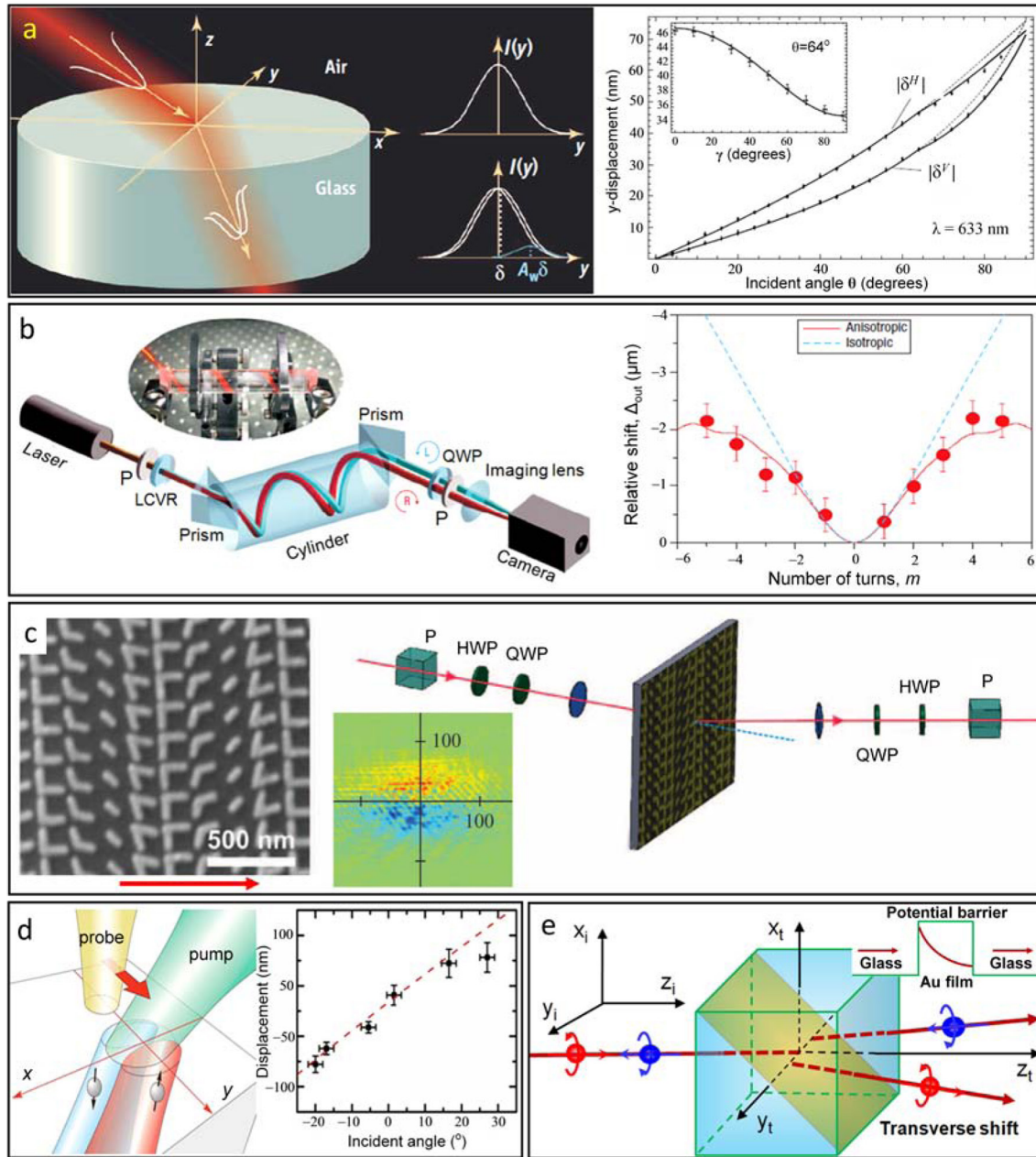


**Figure 1.** Examples of the SHE of light at optical interfaces. (a) Left panel: schematic picture of the SHE of a beam refracting at an air–glass interface. (From [107]; figure reprinted with permission from the AAAS.) Middle top: linearly polarized incident light beam with an initial Gaussian profile  $I(y)$ . Middle bottom: the SHE of light manifesting as a small spin Hall shift  $\delta$  which is boosted by a large factor  $A_w$  in a weak measurement procedure [28]. Right panel: measured results for the spin Hall shifts (maximum  $\sim \lambda/10$ ) with respect to the incident angle  $\theta$ . The inset denotes the shift versus polarization angle  $\gamma$  of the incident beam in a fixed incident angle  $\theta = 64^\circ$ . (From [28]; figure reprinted with permission from the AAAS.) (b) Left panel: direct measurement of the SHE of light in a glass cylinder in which the spin Hall shift accumulates along a helical trajectory. The inset depicts the real picture of the light beam propagating in a helical trajectory. Right panel: the relative spin Hall shift ( $\Delta_{\text{out}}$ ) between the two spin components versus the turns of the helix. The dashed and solid curves are calculated and measured results. (Reprinted by permission from Macmillan Publishers Ltd: Nature Photonics [29], Copyright (2008)). (c) Spin Hall splitting induced by a plasmonic metasurface with a rapidly varying phase discontinuity under normal incidence. Left: metasurface photo captured by a scanning electron microscope (SEM). The red arrow indicates the dynamical phase gradient. Right: experimental setup. The inset depicts the transverse spin accumulation with red and blue separately denoting  $\sigma = +1$  and  $\sigma = -1$  photons. (From [94]; figure reprinted with permission from the AAAS.) (d) Imaging the SHE of light in the air–semiconductor interface. Left: geometry of the model. Right: spin Hall displacements with a good agreement between the calculated (dashed line) and experimental results (cross-shaped symbols) for different incident angles of the probe beam. (Reproduced with permission from [89]. © 2009 Optical Society of America.) (e) Illustration of the spin Hall shift in photon tunneling. A linearly polarized beam transmits across a potential barrier comprising two glass prisms embedded with a gold film, and transversely separates into two circularly polarized beams. (Reprinted by permission from Macmillan Publishers Ltd: Nature Scientific Reports [100], Copyright (2014)). HWP, QWP, P and LCVR denote half-wave plate, quarter-wave plate, polarizer and liquid-crystal variable retardation.

intensively investigated. Qin *et al* have reported the SHE in an air–uniaxial crystal interface and found that the spin Hall shift can be modulated by the direction of the crystal optical axis and the incident angle [87]. By considering the interplay between the spin–orbit interaction and the Goos–Hänchen effect, an in-plane spin separation, which is distinct from the Goos–Hänchen shift and the spin Hall shift, has also been observed in an air–glass interface [101–103]. An inhomogeneous plasmonic metasurface with rapidly varying phase discontinuity has been fabricated to deflect a light beam at normal incidence in which a spin Hall shift was observed by Yin *et al* (figure 1(c)) [94]. Appropriate arrangement of the unit cells with different geometries creates a dynamical phase gradient along the surface of the medium (not a geometric PB phase gradient because the local optical axis direction does not change), and deflects the light beam even at normal incidence. Hence, the observed spin Hall shift occurs in the beam refraction at the air–metasurface interface akin to the SHE in the air–glass interface [28], which essentially originates from the spin redirection RVB phase. Ménard *et al* have demonstrated a general optical pump–probe technology to image the SHE of light in the interface between air and an absorbing semiconductor (GaAs), as depicted in figure 1(d) [89, 90]. The spatial splitting of the spin photons couples to different spins of electrons in the GaAs owing to the transfer of SAM from photons to electrons. This feature can be used to detect the carrier density of the spin electrons by measuring the SHE of light, which bridges the gap between condensed matter physics and the SHE of light. Luo’s group has investigated the SHE in multi-layered nanostructures, metallic films, few-layer graphene and photon tunneling structures [43, 45, 63, 64, 82, 98–100]. They have shown that the spin Hall shift is very sensitive to the optical properties of the interface; hence the shift can be modulated by engineering the interface with appropriate optical parameters, including enhancing or suppressing the SHE or reversing the direction of spin accumulation [43, 82]. In turn, the SHE can be used as an advantageous metrological tool for determining the thickness of metallic and magnetic nano-films, and even atomically thin 2D materials [63, 64, 98]. Photon tunneling is generally regarded as a 2D process, in other words, it only takes place in the incident plane. Investigation of the SHE in photon tunneling structures by Luo *et al* has clarified the three-dimensional nature of the photon tunneling (figure 1(e)) [99, 100]. As shown by Ren *et al* [104] and Qiu *et al* [65], the SHE of light at the interface between air and magnetic films is significantly different from that at air–glass interfaces due to the complex refractive index of magnetic films. Thus, the SHE can be used as a precise and sensitive tool for determining the magnetic-optical constant of magnetic films, which has great potential in magnetic physics.

The above-mentioned SHEs occur for paraxial light beams, depending upon the local wave vector variation in the spatial beam spectrum. They show spin Hall shifts on a subwavelength scale induced by the weak spin–orbit interactions and the RVB phase gradient. In nonparaxial cases, such as in high-numerical-aperture focusing and small-particle scattering, the local wave vector changes more significantly. This indicates the occurrence of enhanced spin–orbit interactions and SHEs

[38–42]. In addition, near the Brewster angle in the beam reflection in air–glass interfaces, the spin Hall shifts show abnormal behaviors. They can reach several wavelengths, which is dozens of times larger than the previously reported SHEs [43–46].

In general, the spatial shift induced by the RVB phase is sometimes accompanied by a transverse angular shift where the axis of the reflected or refracted beam makes a tiny transverse angular deviation from the beam propagation axis defined by Snell’s law and the Fresnel formula [27, 86, 105, 106]. The angular shift is inversely proportional to the beam waist and increases with the propagation distance of the light beam, which is a diffraction phenomenon of beam propagation [27]. It is also a momentum shift, yet totally different from that induced by the PB phase gradient.

The above discussions relating to the transverse shift dealt with polarized light beams with a fundamental-mode Gaussian type. In fact, vortex beams carrying intrinsic OAM [74], for example Laguerre–Gaussian mode beams, have also been considered. In 2001, Fedoseyev theoretically predicted a vortex-induced transverse shift of the centroid of a Laguerre–Gaussian beam in the reflection and refraction at an optical interface [108]. Then the theoretical treatment was extended to a unified form to describe both the longitudinal and transverse shifts of the vortex beam [109–113]. The underlying physics is attributed to the interaction between the intrinsic OAM and extrinsic OAM, that is, the orbit–orbit interaction. In the interfacial reflection and refraction, the intrinsic OAM component in the normal direction changes, and this must be compensated by the extrinsic OAM, i.e. manifesting in a transverse beam shift. It has been demonstrated that the vortex beam shift is accompanied by huge transverse deformation of the beam profiles [110, 114, 115]. Similar to the SHE of light, this effect can be referred to as the OAM Hall effect. Experimental observation of this orbital-dependent transverse shift has also been made [112, 116, 117].

### 3.2. Weak measurements of the SHE of light

Generally, the spin Hall shift occurring at an optical interface is just a few tens of nanometers. The measurement of such a tiny shift is in general challenging since it cannot be directly discriminated with a position sensor or a CCD camera. In 2008, Hosten and Kwiat first employed the quantum weak measurement method to observe the SHE of a light beam refracted at an air–glass interface (as depicted in figure 2(a)) [28]. The experimental results verify the theoretical predictions of Bliokh *et al* [26, 27]. This signal enhancement technique was initially developed by Aharonov *et al* [118] for quantum measurement, and has attracted a lot of attention [119–124]. The quantum weak measurement does not significantly perturb the system in the measurement process, and in this way is unlike traditional projective quantum measurement that strongly perturbs the system being measured [118–124]. Application of the weak measurement technique in the context of optical implementation has increased rapidly in the years since the pioneering work of Hosten and Kwiat. It has been employed to successfully measure nanoscale optical beam

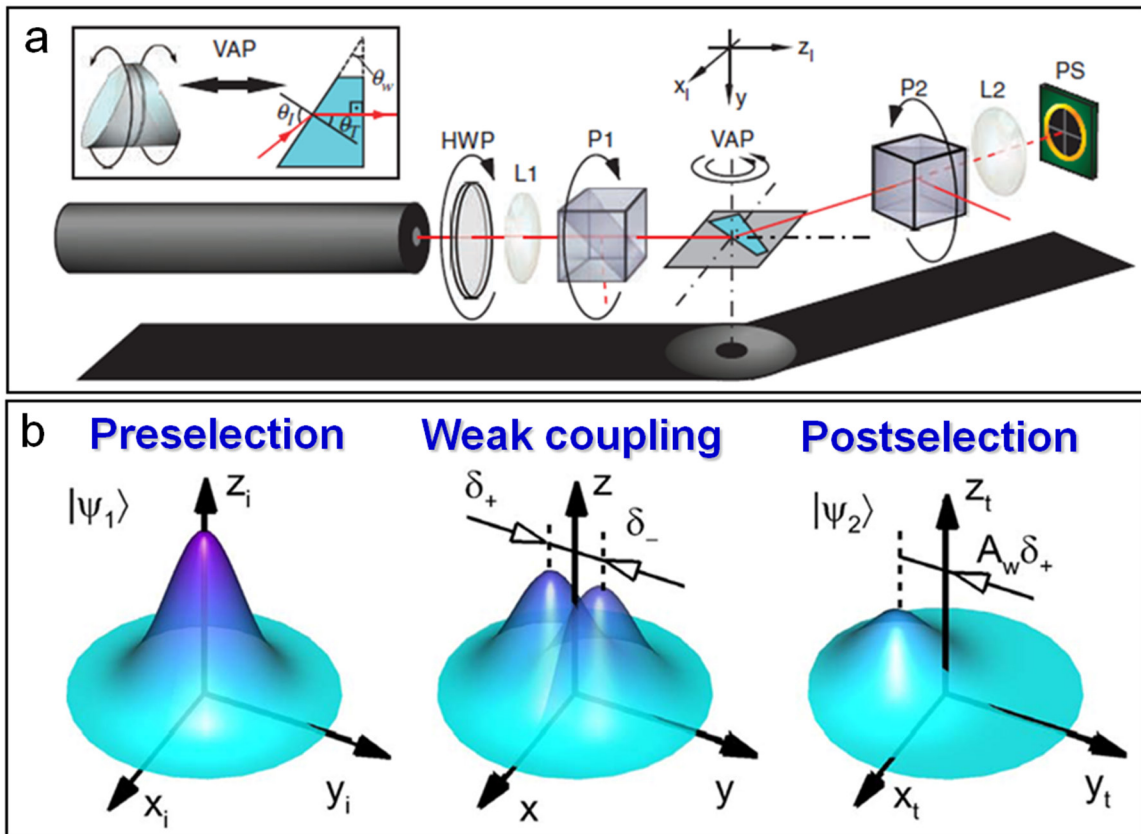


**Figure 2.** Experimental process of weak measurements for detecting the SHE of light. (a) The He–Ne laser source outputs a linearly polarized beam at 633 nm wavelength. A half-wave plate (HWP) is employed to adjust the beam intensity. Two Glan laser polarizers (P1 and P2) pre-select and post-select the states, respectively. The variable angle prism (VAP) refracts the light beam where the spin Hall shift is produced. (From [28]; figure reprinted with permission from the AAAS.) The focal distances of lenses L1 and L2 are 25 and 125 mm, respectively. (b) The system is pre-selected by P1 in state  $|\psi_1\rangle$ . The weak coupling connects the meter with the eigenstates of the measured observable. The system is post-selected in state  $|\psi_2\rangle$  by P2. An interference effect appears in the meter in which the final shift will be amplified  $A_w$  times.  $\delta_{\pm}$  denotes the spin Hall shift for right- and left-handed polarizations. PS, position sensor.

shifts, including the spin Hall shift [28, 43, 44, 63–65, 87, 88, 100–104, 125] and the Goos–Hänchen shift [126, 127].

There are three steps in weak measurements of the SHE of light: pre-selection, weak coupling and post-selection (figure 2(b)). The process of weak measurements for detecting the SHE of light can be described as follows. First, the light beam passes through the first polarizer (P1) being selected as a well-defined pre-selection state. Then, the SHE occurs at the air–glass interface as a weak coupling between the meter and the observable. Finally, another polarizer (P2) is used to post-select the system and obtain the distinguished eigenvalues. Using weak measurements, the SHE of light can be detected with the desired accuracy. Due to the relative transmission direction of the two polarizers, the shift of the post-selected beam can be enhanced significantly for several orders of magnitude. In the experiments, the resolution of displacement reaches  $\sim 1$  Å. In fact, recent research has shown that the maximum weak value and pointer shift could be acquired with an optimal superposition of pre-selection and post-selection states, which offers a possible way to improve the accuracy of weak measurements [128–131].

In fact, the beam shifts can be understood as a classical analogue of quantum weak measurements [132–134]. The

measured beam shifts in weak measurement experiments denote the product of the actual spin Hall shifts and a complex quantum weak value of the photon spin. In this way, the real and imaginary parts of the weak value correspond to the real spatial shift and angular shift of the beam, respectively.

### 3.3. The geometric SHE of light

The geometric SHE of light was proposed by Aiello *et al* in 2009 [135]. The observation of the spin Hall shift in the geometric SHE does not depend upon light–matter interaction; however, it could be observed in an oblique plane with respect to the propagation direction even when a light beam propagates in free space [136, 137]. The geometric SHE is only determined by the geometry of the beam–detector system, hence its name. It can be viewed as a consequence of an effective spin–orbit interaction that generates an effective transverse SAM in the oblique observation plane.

The underlying principle can also be interpreted in terms of an effective geometric phase. Projecting a light beam onto a tilted observation plane, the constituent angular spectrum components acquire different effective polarization ‘rotations’ in  $k$  space. This results in the generation of an effective and

locally varying RVB phase, and thus the geometric SHE. When observed in the plane perpendicular to the propagation axis, the effective ‘rotations’ vanish and no spin-dependent shift can be detected. Until now the geometric SHE has been investigated for collimated paraxial beams, polarizing interfaces, OAM-carrying light beams, tightly focused spin-segmented beams and polarization-tailored synthetic beams [135–141]. It is worth noting that the geometric SHE can also be explained in terms of the relativistic Hall effect for relativistic objects which occurs in free space [142–144]. In this manner, the distribution of energy flow through the tilted observation plane differs from that through the cross section of beam propagation, which manifests as a spin Hall centroid shift.

Unlike the SHE, which occurs at optical interfaces, the geometric SHE intrinsically depends upon the polarization distribution of the beam projected onto a tilted detector instead of any type of light–matter interaction. Similar to the SHE taking place in the reflection and refraction of light at an interface, the geometric spin Hall shift is also extremely weak.

## 4. SHE of light induced by the PB phase

### 4.1. SHE of light in structured anisotropic media

The PB phase was first discovered by Pancharatnam in 1956 in optics, and revisited and generalized to other physics by Berry in 1984 [48–52]. Now it is a fundamental concept in physics. In optics, it is relative to the manipulation of the polarization state of light. When a light beam propagates through a birefringent wave plate, it can acquire a PB phase relying only on the orientation of the optical axis in addition to the dynamical phase originating from the optical path difference [83]. Provided the wave plate exhibits a space-variant optical axis orientation, it can imprint the light beam with a spatially varying PB phase which forms a PB phase gradient [53–62]. A subwavelength dielectric grating has been fabricated in the infrared range to structure an inhomogeneous anisotropic medium with constant retardation and gradually varying effective optical axis orientation [58]. It can behave as a PB phase element and be employed to generate inhomogeneously polarized beams or function as a polarization beam splitter or an optical switch. A liquid-crystal  $q$ -plate is another kind of PB phase element which can operate in the visible range [55, 56]. It is made of nematic liquid-crystal molecules, whose local optical axes are made to vary in the azimuthal direction by controlling the external electric field. The  $q$ -plate can be employed to modulate the intrinsic OAM of light and functions as a generator of vortex and vector beams.

The PB phase gradient is spin-dependent in nature and may result in a spin Hall momentum shift. In 2011, Shitrit *et al* observed a one-dimensional (1D) spin Hall momentum shift in periodic plasmonic chains (period  $a$ ) comprising a string of plasmonic nano-apertures (see figure 3(a)) [60]. They actually form an effective inhomogeneous anisotropic medium in one direction (the  $x$  direction). A light beam passing through a medium with spatially inhomogeneous anisotropy exhibits a tight analogy with scattering of a temporally rotating wave plate [52]. Hence the spatial evolution of the locally varying,

effective optical axes of the plasmonic nano-apertures resembles the temporal evolution of a revolving anisotropic medium. Because of the gradually varying direction of the local optical axes, a circularly polarized light beam ( $\sigma_{\text{in}} = \pm 1$ ) reverses its handedness ( $\sigma_{\text{out}} = \mp 1$ ) after passing through this nanostructure and acquires a locally varying PB phase which forms a gradient, and thus brings about a spin-dependent momentum shift of  $\Delta k_x = 2\sigma_{\text{out}}\pi/a$ . In this process the SAM of light partially converts into intrinsic OAM [53–57]. The amount of conversion is determined by the retardation of the medium. The spin Hall momentum splitting can be directly detected by measuring the Stokes parameter  $S_3$  with the combined use of a quarter-wave plate, a linear polarizer and a CCD camera [60], because the  $S_3$  parameter can be used to characterize the degree of circular polarization of light and the spin accumulation of photons [84].

Recently, the observation of spin Hall momentum shifts in inhomogeneous 1D or 2D metamaterials/metasurfaces has also been reported [62, 145–151]. Metamaterials and metasurfaces are human-made materials which are engineered to generate almost any conceivable electromagnetic properties, even including those undiscovered in nature [152–157]. They have shown considerable potential in manipulation of SAM, OAM and the SHE of light, thereby offering convenient opportunities for the development of spin-controllable photonics and photonic spin Hall devices.

It is expected that the two spin components will focus and defocus, respectively, provided that the PB phase gradient is in the radial direction [59, 158–160]. This indicates that the spin Hall momentum shift will occur in the radial direction. Bhandari theoretically proposed achievement of a geometric phase lens using an inhomogeneous wave plate with a radially varying optical axis direction [158]. Hasman *et al* have experimentally shown the formation of a quantized PB phase optical element using a computer-generated locally varying subwavelength grating fabricated on a dielectric base under infrared radiation [59]. This PB phase element can realize a spin-dependent focusing lens that focuses one spin component and defocuses the other, enabling approaches for spin-controlled optical elements.

If the local optical axes vary in the azimuth direction, the PB phase gradient is also in this direction, which results in an azimuthal SHE of light with rotational symmetry. Making a light beam pass through such a medium at normal incidence, one can find that the resultant beam has a hybrid polarization distribution in the transverse plane. Under the condition of incomplete conversion of SAM to intrinsic OAM, the spin-dependent splitting and spin accumulation of photons may be detected by measuring the Stokes parameter  $S_3$  of the resultant beam, which manifests as rotational symmetry with alternative right- and left-handed spin photon accumulations [161–164]. For complete conversion, the medium can serve as a vortex beam generator or vector beam generator, depending upon the polarization of the incident beam [53–57].

### 4.2. SHE of light in symmetry breaking

In solids, under broken inversion symmetry, the spin-orbit interaction of relativistic electrons results in

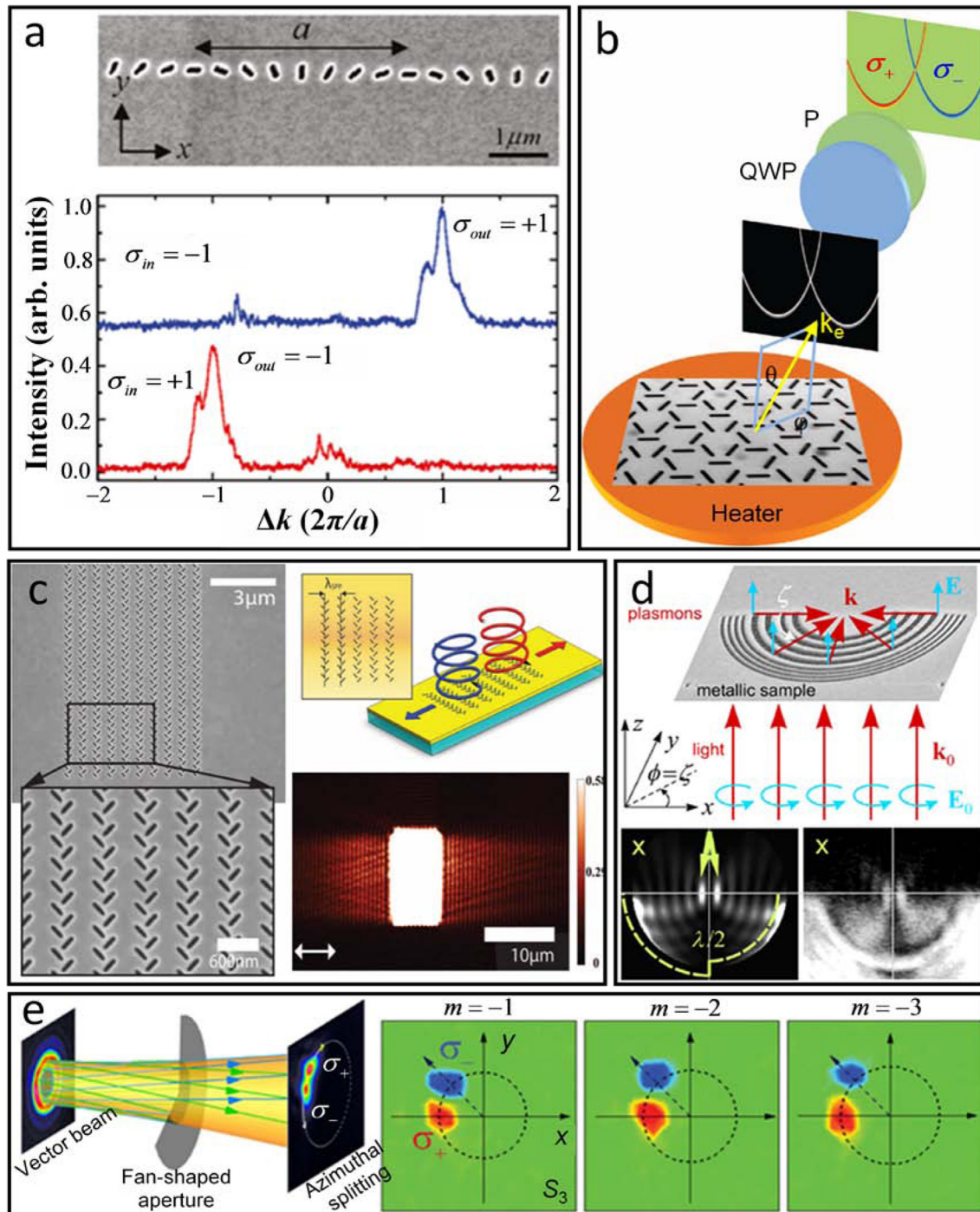


**Figure 3.** Examples of the SHE induced by the PB phase. (a) Spin Hall momentum offset in a plasmonic chain. Top: SEM photo of a plasmonic chain. Local orientation of the nano-aperture changes slightly along the  $x$  direction with a spatial rotation period of  $a$ . Bottom: the spin Hall momentum offset. (Reprinted with permission from [60]. Copyright (2011) American Chemical Society.) (b) Observation of the spin-polarized momentum shift in a spinoptical metasurface by measuring the intensity dispersion of the thermal radiation. QWP, quarter-wave plate; P, polarizer. (From [61]; figure reprinted with permission from the AAAS.) (c) Controllable spin-direction coupling between light and surface plasmonic polaritons in an inversion asymmetric plasmonic metasurface. Left: SEM image of a structure fabricated in a gold film for operation at 633 nm wavelength. Top right: schematic illustration of the spin Hall shift of surface plasmonic polaritons. Bottom right: near-field scanning optical microscopy of the structure under linearly polarized radiation. (From [71]; figure reprinted with permission from the AAAS.) (d) Spin Hall momentum shift of surface plasmonic waves. Top: scheme of the experiment. Bottom right and left: the simulated and experimental results of the spin Hall splitting of the surface plasmons illuminated by a linearly polarized beam. (Reprinted figure with permission from [52], Copyright (2008) by the American Physical Society.) (e) SHE of cylindrical vector beam with rotational symmetry broken. Left: schematic illustration of vector beam blocking by a fan-shaped aperture. Right: experimental results of the spin Hall splitting of the vector beams with different polarization geometries (topological charge  $m = -1, -2$  and  $-3$ ). Here, three-quarters of the vector beam is obstructed by the aperture. (Figure reprinted with permission from [41]. Copyright 2014, AIP Publishing LLC.)

momentum-dependent Rashba spin splitting, where the spin-degeneracy of the energy dispersion of an electronic state is removed [165]. In valleytronics, inversion symmetry breaking can give rise to a valley-dependent transverse shift of carriers in momentum space, manifesting as the valley Hall effect [11–13]. Similar Rashba spin splitting has also been observed in thermal emission emitted from a spatially varying antenna lattice with inversion asymmetry [166, 167]. The photonic version of spin-dependent momentum splitting in inversion symmetry breaking associated with the geometric PB phase was recently presented in spinoptical metasurfaces [61, 168, 169]. In 2013, Shitrit *et al* demonstrated a spin-controlled optical mode of spinoptical metasurfaces arising from spatial inversion symmetry breaking (figure 3(b)) [61]. The inversion asymmetric metasurface is obtained by standard photolithographic technology via etching an anisotropic optical antenna array on a SiC substrate whose orientation angle is space-variant. It is very similar to the role of the potential gradient played in the electronic Rashba effect and produces a spin-split dispersion of photons, manifesting as a spin Hall momentum offset. Hence, the design of the spinoptical metasurface with appropriate symmetry properties offers a promising route for spin-based nanophotonic applications. As reported by Lin *et al*, an inversion-symmetry broken plasmonic metasurface can be used to modulate the direction of the spin-controlled surface plasmons (figure 3(c)) [71]. The different spin states of the incident beam couple to opposite directions of the surface plasmons, enabling realization of a spin-dependent plasmonic coupler.

The spin-orbit interaction in rotational symmetry breaking can also result in spin-dependent momentum splitting. In 2008, the Hasman group showed a spin-based plasmonic effect in plasmonic nanostructures (figure 3(d)) [52, 70, 170]. In annular subwavelength metallic gratings, a PB phase-based plasmonic vortex can be generated, the handedness of which relies on the polarization state of the incident beam. Being an overlap of the right- and left-handed circular modes, a linearly polarized incident beam brings about a spin Hall splitting of the surface plasmons in a semi-annular grating, i.e. the SHE of surface plasmons. The semi-annular grating can be regarded as a case of breaking the rotational symmetry of the annular grating.

The SHE of light in  $q$ -plate-like metamaterials or metasurfaces with broken rotational symmetry has been investigated theoretically and experimentally by Kang *et al* and Liu *et al* independently [171, 172]. Two ways were suggested to break the rotational symmetry of the azimuthal-gradient materials. The first is to scrub a sector of the  $q$ -plate-like structure and hold the remainder. The second is to displace the incident beam from the center of rotation of the structure. The metastructure used in the work of Liu *et al* is all-dielectric, and may therefore exhibit relatively higher transmission efficiency and lower loss. It is worth noting that 1D inhomogeneous anisotropic structures can be viewed as a result of unfolding the 2D  $q$ -plate-like geometry from polar to Cartesian coordinates [60, 62, 145–151, 168]. It is also a type of rotational symmetry breaking.

Owing to the close relationship between the SHE and manipulation of the polarization of light, breaking the rotational symmetry of a linearly polarized vector beam (see [173]

for a review of vector beam) can lead to observation of a spin Hall shift in the azimuthal direction (figure 3(e)) [41, 174, 175]. The vector beam can be viewed as the overlap of two circularly polarized beams with exactly opposite handedness and opposite helical phases [176, 177]. Obstructing part of the vector beam by a sector aperture breaks the beam's rotational symmetry, and enables observation of the spin accumulation of photons at the beam edge. The two spin components of the vector beam carry spin-dependent vortex phases which are very similar to the geometric PB phases produced by the  $q$ -plate-like media. Under broken rotational symmetry, the opposite azimuthal energy flows of the two components are no longer continuous [178–181] and thus result in the azimuthal spin Hall shift.

## 5. Applications of the SHE of light

Research into the SHE of light has led to a range of applications. One of most interesting applications is in precision metrology. Remarkably, the spin Hall shift in the SHE is sensitive to variations in optical parameters (e.g. refractive indices and thickness). A quantitative relationship between the spin Hall shift and the optical parameters should first be established. After measuring the spin-dependent shifts with weak measurement technology, the physical parameters can be determined with the desirable accuracy. Recently, much progress has been made in this field. The SHE of light was first employed to measure the thickness of metallic nano-films [64]. Similarly, the magneto-optical constant of magnetic films can be determined by measuring the amplified shifts in the SHE of light [65]. It has been demonstrated that the SHE of light can serve as a useful metrological tool for characterizing the layer numbers of 2D materials such as graphene (see [182] for a review of graphene), due to their sensitive dependence on spin Hall shifts [63]. There have already been some methods to determine the layer numbers in a graphene film, but they have limitations [183, 184]. The experimental setup for detecting the spin Hall shift of light reflected at the graphene sample is depicted in figure 4(a). First, using the refractive index data for graphene, the number of layers in a graphene sample can be quickly identified by comparing the experimental results with the theoretical ones (figure 4(a), top right), without any disturbance to the sample. In this case the actual number of layers in graphene can be identified as three because the experimental data agree well with theory for three-layered graphene. As a comparison, Raman spectroscopy of the sample verifies the number of layers as three (figure 4(a), bottom right).

The successful alliance of the SHE of light with plasmonic nanostructures or metamaterials/metasurfaces opens an exciting pathway for developing plasmonic/photonic spin Hall devices, and is leading to a new research field of optics, namely spinoptics [29, 60–62, 70, 168–170, 185, 186]. Gorodetski *et al* have shown a spin-dependent plasmonic lens based on a semi-annular metallic grating [70]. When a right- or left-handed circularly polarized beam impinges onto the grating, the launched surface plasmons imprinted by different geometric phases focus on different positions depending on the handedness of the circular polarization. If a linearly polarized light beam illuminates the structure, the surface

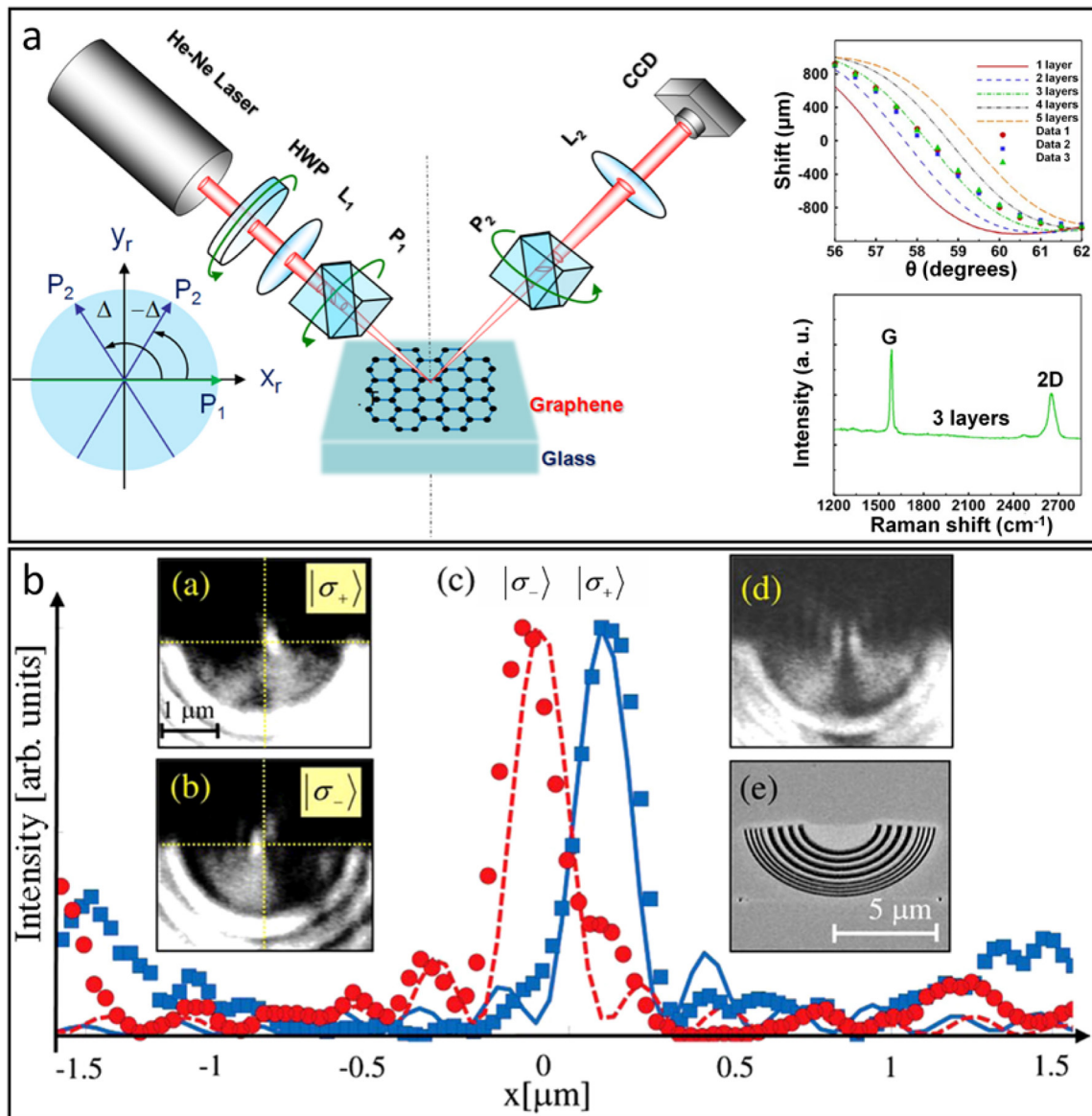


**Figure 4.** Examples of applications of the SHE of light. (a) Identifying the layers of graphene via weak measurement of the spin Hall shift. Left: experimental apparatus for weak measurement of the reflected light of a few-layer graphene sample located on a glass base. HWP, half-wave plate;  $P_{1(2)}$  and  $L_{1(2)}$  denote polarizers and lenses, respectively; CCD, charge-coupled device. The laser outputs a linearly polarized beam. The inset characterizes the pre-selection and post-selection with the two polarizers, separately. Top right: calculated and experimentally measured spin-Hall shift of the graphene sample as functions of the incident angle  $\theta$  with layer numbers varying from one to five. Data 1, 2, and 3 separately indicate the results measured from three different positions of the sample. Bottom right: Raman spectroscopy of the graphene sample. (Reprinted with permission from [63]. Copyright 2012, AIP Publishing LLC.) (b) The PB phase-based plasmonic lens. Top left and bottom left: near-field scanning optical microscope images of the semi-annular plasmonic grating for left- and right-handed radiation, separately. Middle: transverse intensity profiles in the focal plane of the plasmonic lens. Top right: the intensity distribution detected by a near-field scanning optical microscope for linear polarization illumination. Bottom right: SEM of the plasmonic lens. (Reprinted figure with permission from [70], Copyright (2008) by the American Physical Society.)

plasmons manifest as two independent intensity patterns (see figures 3(d) and 4(b)). In this case, the grating can function as a spin-dependent surface plasmon splitter. An inversion asymmetric plasmonic metasurface has also been demonstrated which has the potential to be developed into a spin-dependent plasmonic coupler (figure 3(c)) [71]. Using this structure, the spin information or the spin-encoded photon qubits can be encoded into the surface plasmonic polaritons. Because of the flexible adjustability of the plasmonic grating and metasurface, there is considerable potential for numerous spin-based photonics and plasmonic devices and future on-chip photonic

circuits. Compared with the plasmonic metasurfaces, all-dielectric metasurfaces exhibit a higher transmission efficiency, enabling realization of high-quality transmission-type optical devices [156]. A spin-dependent lens has been realized by integrating a PB phase lens into a conventional plano-convex lens [187]. The integrated lens was fabricated by intense laser writing of self-assembled nano-gratings (acting as a PB phase lens) inside a plano-convex lens. By employing both the PB phase and a dynamical phase (produced by the plano-convex lens per se) to control the wave front, it can focus right- and left-handed light into two different focal points, respectively.

## 6. Conclusions and prospects

We have presented a brief review on recent advances in the SHE of light. The underlying physics of the SHE comes from the spin-orbit interaction of light, which can also be explained in terms of the RVB and PB geometric phases [17, 23–29, 52, 62]. The RVB phase is related to variation of the direction of propagation of light. Typically, when a plane wave reflects and refracts at an optical interface, its polarization vector experiences a rotation, i.e. it acquires a geometric RVB phase in addition to the dynamical phase. Hence, if the plane wave is substituted by a finite-sized beam that comprises many plane waves with slightly different propagation directions, the light beam will obtain an inhomogeneous RVB phase that forms an RVB phase gradient in momentum space. This gradient manifests as a spin Hall shift in real space. On the other hand, the PB phase is associated with manipulation of the polarization of light. If a beam transmits through a birefringent wave plate at normal incidence it acquires a PB geometric phase in addition to the dynamical phase. Supposing that the wave plate exhibits spatially varying optical axis directions (with uniform retardation), then the light beam obtains space-variant PB phases that construct a PB phase gradient in real space resulting in a spin Hall momentum shift.

The spin Hall shift induced by the RVB phase is generally very small (subwavelength scale); however, it can be observed by an indirect method, namely weak measurement technology. This shift is very sensitive to the physical properties (refractive index, thickness, etc) of the media comprising the interface; hence, conversely, the SHE offers a possible avenue to measure or determine the optical parameters of nanostructures such as metallic films, 2D material films and magnetic films [63–65, 98]. In this sense, the SHE of light can be developed into a sensitive and precise tool for studying the physical properties of nanoscale structures.

The spin Hall shift induced by the PB phase occurs in momentum space and increases with propagation distance, so the shift can be directly detected by measuring the Stokes parameter  $S_3$  since it can describe the spin accumulations of photons. The PB phase and the induced SHE can be modulated by designing a metamaterial/metamaterial surface or a plasmonic nano-structure with appropriate structural geometry, enabling the spin states of the photon to be controlled, and paving the way to planar integrated photonic/plasmonic spin Hall components [58–62, 70, 71, 170, 185–187].

It is worth mentioning that a new type of SHE for evanescent and surface modes of light, named the quantum SHE of light, has been proposed recently [16]. It has a purely classical origin, and is formally akin to the quantum SHE for electrons in topological insulators. This effect is based on the fact that evanescent and surface waves exhibit extraordinary transverse SAM directed along the direction orthogonal to the propagation axis [18, 188–191] compared with the longitudinal SAM of propagation waves. The transverse SAM can be seen as a manifestation of the spin-orbit interaction of light; however, it has nothing to do with the geometric Berry phase and results directly from the transversality condition of electromagnetic waves [18, 188, 189]. Importantly, owing to the transversality condition, the direction of the transverse SAM is locked

with the propagation direction of the evanescent wave, i.e. oppositely propagating waves carry exactly opposite transverse SAM. Very recently, the transverse SAM and transverse spin-dependent optical force have been directly measured using a nano-cantilever immersed in an evanescent optical field created by the total internal reflection of a glass surface [192]. Until now, this spin-direction locking characteristic has been discussed in various systems that support evanescent-tail modes, such as metal nanostructures [193, 194], nano-fibers [195, 196], semiconductor nanowires [197] and various waveguides [198–201], which could potentially be applied in spin-controlled plasmonic devices and quantum-optical devices.

In the future, the development of the SHE of light and the evolution of the corresponding spin Hall devices will be continuously pushed forward. Existing research is mainly focused on exploring the SHE of light in different physical systems. More attention should now be paid to designing or engineering a controllable spin Hall shift by tailoring the structure geometry of artificial materials (e.g. metamaterials/metamaterial surfaces and subwavelength nanostructures) for the approaching spin-based photonic/plasmonic applications. Similar to the SHE of light, the OAM Hall effect, making use of the orbital degree of freedom of photons, will lead to the realization of orbit-dependent photonic Hall devices [109, 110]. The pioneering research into the SHE of light in semiconductors has opened a possible avenue to investigate semiconductors using the SHE of light, which establishes a link between semiconductor spintronics and spinoptics [89, 90]. As the SHEs in optics, spintronics, valleytronics, condensed matter physics and high-energy physics share the same physics of spin-orbit interaction in their respective contexts [29, 67, 68], the exploration of the SHE in optics may provide not only a new degree of freedom for controlling photons, thereby further pushing forward the development of photonic spin Hall devices, but also a direct analogy for the SHE in those systems. The results observed for the SHE of light could be generalized to those systems where observation of the SHE is challenging. More interestingly, recent progress made in valleytronics has suggested that valley polarization can be controlled by the SAM of photons, which bridges the gap between photon spin and valleytronics [202, 203].

## Acknowledgments

The work by X Ling is partially supported by the Natural Science Foundation of China (11447010 and 11604087), the Natural Science Foundation of Hunan Province (2015JJ3026), the Science and Technology Plan Project of Hunan Province (2016TP1020) the Excellent Talents Program of HYNNU, and the visiting scholar program of the China Scholarship Council. C.W.Q. would like to acknowledge financial support from A\*STAR under the Pharos Program (1527000014) and the National University of Singapore (R-263-000-A45-112).

## References

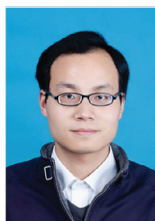
- [1] Hall E H 1879 On a new action of the magnet on electric currents *Am. J. Math.* **2** 287–92
- [2] Nagaosa N, Sinova J, Onoda S, MacDonald A H and Ong N P 2010 Anomalous Hall effect *Rev. Mod. Phys.* **82** 1539–82

- [3] Haldane F D M 1988 Model for a quantum Hall effect without Landau levels: condensed-matter realization of the ‘parity anomaly’ *Phys. Rev. Lett.* **61** 2015–8
- [4] Ezawa Z F 2013 *Quantum Hall Effects: Recent Theoretical and Experimental Developments* (Singapore: World Scientific)
- [5] Hirsch J E 1999 Spin Hall effect *Phys. Rev. Lett.* **83** 1834–7
- [6] Kato Y K, Myers R C, Gossard A C and Awschalom D D 2004 Observation of the spin Hall effect in semiconductors *Science* **306** 1910–3
- [7] Sinova J, Culcer D, Niu Q, Sinitsyn N A and Jungwirth T 2004 Universal intrinsic spin Hall effect *Phys. Rev. Lett.* **92** 126603
- [8] Kane C L and Mele E J 2005 Quantum spin Hall effect in graphene *Phys. Rev. Lett.* **95** 226801
- [9] Qi X L and Zhang S C 2010 The quantum spin Hall effect and topological insulators *Phys. Today* **63** 33–8
- [10] Chang C Z *et al* 2013 Experimental observation of the quantum anomalous Hall effect in a magnetic topological insulator *Science* **340** 167–70
- [11] Rycerz A, Tworzydło J and Beenakker C W J 2007 Valley filter and valley valve in graphene *Nat. Phys.* **3** 172–5
- [12] Xiao D, Yao W and Niu Q 2007 Valley-contrasting physics in graphene: magnetic moment and topological transport *Phys. Rev. Lett.* **99** 236809
- [13] Mak K F, McGill K L, Park J and McEue P L 2014 The valley Hall effect in MoS<sub>2</sub> transistors *Science* **344** 1489–92
- [14] Carusotto I and Ciuti C 2013 Quantum fluids of light *Rev. Mod. Phys.* **85** 299–366
- [15] Mittal S *et al* 2014 Topologically robust transport of photons in a synthetic gauge field *Phys. Rev. Lett.* **113** 087403
- [16] Bliokh K Y, Smirnova D and Nori F 2015 Quantum spin Hall effect of light *Science* **348** 1448–51
- [17] Bliokh K Y, Rodríguez-Fortuño F J, Nori F and Zayats A V 2015 Spin-orbit interactions of light *Nat. Photon.* **9** 796–808
- [18] Bliokh K Y and Nori F 2015 Transverse and longitudinal angular momenta of light *Phys. Rep.* **592** 1–38
- [19] Wolf S A *et al* 2001 Spintronics: a spin-based electronics vision for the future *Science* **294** 1488–95
- [20] Awschalom D D and Flatté M E 2007 Challenges for semiconductor spintronics *Nat. Phys.* **3** 153–9
- [21] Chappert C, Fert A and Van Dau F N 2007 The emergence of spin electronics in data storage *Nat. Mater.* **6** 813–23
- [22] Wunderlich J *et al* 2010 Spin Hall effect transistor *Science* **330** 1801–4
- [23] Bliokh K Y and Bliokh Y P 2004 Modified geometrical optics of a smoothly inhomogeneous isotropic medium: the anisotropy, Berry phase, and the optical Magnus effect *Phys. Rev. E* **70** 026605
- [24] Bliokh K Y and Bliokh Y P 2004 Topological spin transport of photons: the optical Magnus effect and Berry phase *Phys. Lett. A* **333** 181–6
- [25] Onoda M, Murakami S and Nagaosa N 2004 Hall effect of light *Phys. Rev. Lett.* **93** 083901
- [26] Bliokh K Y and Bliokh Y P 2006 Conservation of angular momentum, transverse shift, and spin Hall effect in reflection and refraction of an electromagnetic wave packet *Phys. Rev. Lett.* **96** 073903
- [27] Bliokh K Y and Bliokh Y P 2007 Polarization, transverse shifts, and angular momentum conservation laws in partial reflection and refraction of an electromagnetic wave packet *Phys. Rev. E* **75** 066609
- [28] Hosten O and Kwiat P 2008 Observation of the spin Hall effect of light via weak measurements *Science* **319** 787–90
- [29] Bliokh K Y, Niv A, Kleiner V and Hasman E 2008 Geometrodynamics of spinning light *Nat. Photon.* **2** 748–53
- [30] Nori F 2008 The dynamics of spinning light *Nat. Photon.* **2** 716–7
- [31] Fedorov F I 1955 To the theory of total reflection *Dokl. Akad. Nauk SSR* **105** 465–68
- [32] Imbert C 1972 Calculation and experimental proof of the transverse shift induced by total internal reflection of a circularly polarized light beam *Phys. Rev. D* **5** 787–95
- [33] Dooghin A V, Kundikova N D, Liberman V S and Zel’dovich B Y 1992 Optical Magnus effect *Phys. Rev. A* **45** 8204–8
- [34] Liberman V S and Zel’dovich B Y 1992 Spin-orbit interaction of a photon in an inhomogeneous medium *Phys. Rev. A* **46** 5199–207
- [35] Schilling H 1965 Die Strahlversetzung bei der Reflexion linear oder elliptisch polarisierter ebener Wellen an der Trennebene zwischen absorbierenden Medien *Ann. Phys.* **16** 122–34
- [36] Player M A 1987 Angular momentum balance and transverse shifts on reflection of light *J. Phys. A: Math. Gen.* **20** 3667–78
- [37] Fedoseyev V G 1988 Conservation laws and transverse motion of energy on reflection and transmission of electromagnetic waves *J. Phys. A: Math. Gen.* **21** 2045–59
- [38] Haefner D, Sukhov S and Dogariu A 2009 Spin Hall effect of light in spherical geometry *Phys. Rev. Lett.* **102** 123903
- [39] Rodríguez-Herrera O G, Lara D, Bliokh K Y, Ostrovskaya E A and Dainty C 2010 Optical nanoprobeing via spin-orbit interaction of light *Phys. Rev. Lett.* **104** 253601
- [40] Roy B, Ghosh N, Banerjee A, Gupta S D and Roy S 2014 Manifestations of geometric phase and enhanced spin Hall shifts in an optical trap *New J. Phys.* **16** 083037
- [41] Ling X *et al* 2014 Realization of tunable spin-dependent splitting in intrinsic photonic spin Hall effect *Appl. Phys. Lett.* **105** 151101
- [42] Kruk S S *et al* 2014 Spin-polarized photon emission by resonant multipolar nanoantennas *ACS Photonics* **1** 1218–23
- [43] Luo H, Zhou X, Shu W, Wen S and Fan D 2011 Enhanced and switchable spin Hall effect of light near the Brewster angle on reflection *Phys. Rev. A* **84** 043806
- [44] Kong L *et al* 2012 Spin Hall effect of reflected light from an air-glass interface around the Brewster’s angle *Appl. Phys. Lett.* **100** 071109
- [45] Ling X, Luo H, Tang M and Wen S 2012 Enhanced and tunable spin Hall effect of light upon reflection of one-dimensional photonic crystal with a defect layer *Chin. Phys. Lett.* **29** 074209
- [46] Götte J B and Dennis M R 2013 Limits to superweak amplification of beam shifts *Opt. Lett.* **38** 2295–7
- [47] Slobozhanyuk A P *et al* 2016 Enhanced photonic spin Hall effect with subwavelength topological edge states *Laser Photon. Rev.* **10** 656–64
- [48] Berry M V 1984 Quantal phase factors accompanying adiabatic changes *Proc. R. Soc. A* **392** 45–57
- [49] Pancharatnam S 1956 Generalized theory of interference, and its applications *Proc. Indian Acad. Sci. A* **44** 247–62
- [50] Edited by Shapere A and Wilczek F 1989 *Geometric Phase in Physics* (Singapore: World Scientific)
- [51] Bhandari R 1997 Polarization of light and topological phases *Phys. Rep.* **281** 1–64
- [52] Bliokh K Y, Gorodetski Y, Kleiner V and Hasman E 2008 Coriolis effect in optics: unified geometric phase and spin-Hall effect *Phys. Rev. Lett.* **101** 030404
- [53] Bomzon Z, Kleiner V and Hasman E 2001 Pancharatnam–Berry phase in space-variant polarization-state manipulations with subwavelength gratings *Opt. Lett.* **26** 1424–6
- [54] Biener G, Niv A, Kleiner V and Hasman E 2002 Formation of helical beams by use of Pancharatnam–Berry phase optical elements *Opt. Lett.* **27** 1875–7
- [55] Marrucci L, Manzo C and Paparo D 2006 Optical spin-to-orbital angular momentum conversion in inhomogeneous anisotropic media *Phys. Rev. Lett.* **96** 163905

- [56] Marrucci L, Manzo C and Paparo D 2006 Pancharatnam–Berry phase optical elements for wavefront shaping in the visible domain: switchable helical modes generation *Appl. Phys. Lett.* **88** 221102
- [57] Karimi E *et al* 2014 Generating optical orbital angular momentum at visible wavelengths using a plasmonic metasurface *Light: Sci. Appl.* **3** e167
- [58] Hasman E, Bomzon Z, Niv A, Biener G and Kleiner V 2002 Polarization beam-splitters and optical switches based on space-variant computer-generated subwavelength quasi-periodic structures *Opt. Commun.* **209** 45–54
- [59] Hasman E, Kleiner V, Biener G and Niv A 2003 Polarization dependent focusing lens by use of quantized Pancharatnam–Berry phase diffractive optics *Appl. Phys. Lett.* **82** 328–30
- [60] Shitrit N, Bretner I, Gorodetski Y, Kleiner V and Hasman E 2011 Optical spin Hall effects in plasmonic chains *Nano Lett.* **11** 2038–42
- [61] Shitrit N, Yulevich I, Maguid E, Ozeri D, Veksler D, Kleiner V and Hasman E 2013 Spin-optical metamaterial route to spin-controlled photonics *Science* **340** 724–26
- [62] Ling X *et al* 2015 Giant photonic spin Hall effect in momentum space in a structured metamaterial with spatially varying birefringence *Light: Sci. Appl.* **4** e290
- [63] Zhou X, Ling X, Luo H and Wen S 2012 Identifying graphene layers via spin Hall effect of light *Appl. Phys. Lett.* **101** 251602
- [64] Zhou X, Xiao Z, Luo H and Wen S 2012 Experimental observation of the spin Hall effect of light on a nanometal film via weak measurements *Phys. Rev. A* **85** 043809
- [65] Qiu X *et al* 2014 Determination of magneto-optical constant of Fe films with weak measurements *Appl. Phys. Lett.* **105** 131111
- [66] Stone M 2015 Topology, spin, and light *Science* **348** 1432–3
- [67] Bérard A and Mohrbach H 2006 Spin Hall effect and Berry phase of spinning particles *Phys. Lett. A* **352** 190–5
- [68] Gosselin P, Bérard A and Mohrbach H 2007 Spin Hall effect of photons in a static gravitational field *Phys. Rev. D* **75** 084035
- [69] Murakami S 2015 Berry curvature and topological phases for electrons, photons, and magnons *JPS Conf. Proc.* **4** 011001
- [70] Gorodetski Y, Niv A, Kleiner V and Hasman E 2008 Observation of the spin-based plasmonic effect in nanoscale structures *Phys. Rev. Lett.* **101** 043903
- [71] Lin J *et al* 2013 Polarization-controlled tunable directional coupling of surface plasmon polaritons *Science* **340** 331–4
- [72] Kavokin A, Malpuech G and Glazov M 2005 Optical spin Hall effect *Phys. Rev. Lett.* **95** 136601
- [73] Leyder C *et al* 2007 Observation of the optical spin Hall effect *Nat. Phys.* **3** 628–31
- [74] Allen L, Barnett S M and Padgett M J 2003 *Optical Angular Momentum* (Bristol: IOP Publishing)
- [75] Yao A M and Padgett M J 2011 Orbital angular momentum: origins, behavior and applications *Adv. Opt. Photonics* **3** 161–204
- [76] Andrews D L and Babiker M 2013 *The Angular Momentum of Light* (Cambridge: Cambridge University Press)
- [77] Aharonov Y and Anandan J 1987 Phase change during a cyclic quantum evolution *Phys. Rev. Lett.* **58** 1593–6
- [78] Samuel J and Bhandari R 1988 General setting for Berry’s phase *Phys. Rev. Lett.* **60** 2339–42
- [79] Jordan T F 1988 Berry phases for partial cycles *Phys. Rev. A* **38** 1590–2
- [80] Chiao R Y and Wu Y S 1986 Manifestations of Berry’s topological phase for the photon *Phys. Rev. Lett.* **57** 933–6
- [81] Berry M V 1987 The adiabatic phase and Pancharatnam’s phase for polarized light *J. Mod. Opt.* **34** 1401–7
- [82] Luo H *et al* 2011 Enhancing or suppressing the spin Hall effect of light in layered nanostructures *Phys. Rev. A* **84** 033801
- [83] Courtial J 1999 Wave plates and the Pancharatnam phase *Opt. Commun.* **171** 179–83
- [84] Born M and Wolf E 1999 *Principles of Optics* (Cambridge: Cambridge University Press)
- [85] Goos F and Hänchen H 1947 Ein neuer und fundamentaler Versuch zur Totalreflexion *Ann. Phys.* **1** 333–46
- [86] Bliokh K Y and Aiello A 2013 Goos–Hänchen and Imbert–Fedorov beam shifts: an overview *J. Opt.* **15** 014001
- [87] Qin Y *et al* 2010 Spin Hall effect of reflected light at the air–uniaxial crystal interface *Opt. Exp.* **18** 16832–9
- [88] Bliokh K Y *et al* 2016 Spin-Hall effect and circular birefringence of a uniaxial crystal plate *Optica* **3** 1039–47
- [89] Ménard J M, Mattacchione A E, Betz M and van Driel H M 2009 Imaging the spin Hall effect of light inside semiconductors via absorption *Opt. Lett.* **34** 2312–4
- [90] Ménard J M, Mattacchione A E, van Driel H M, Hautmann C and Betz M 2010 Ultrafast optical imaging of the spin Hall effect of light in semiconductors *Phys. Rev. B* **82** 045303
- [91] Hermosa N, Nugrowati A M, Aiello A and Woerdman J P 2011 Spin Hall effect of light in metallic reflection *Opt. Lett.* **36** 3200–2
- [92] Luo H *et al* 2009 Spin Hall effect of a light beam in left-handed materials *Phys. Rev. A* **80** 043810
- [93] Wang H and Zhang X 2011 Unusual spin Hall effect of a light beam in chiral metamaterials *Phys. Rev. A* **83** 053820
- [94] Yin X, Ye Z, Rho J, Wang Y and Zhang X 2013 Photonic spin Hall effect at metasurfaces *Science* **339** 1405–7
- [95] Kapitanova P V *et al* 2014 Photonic spin Hall effect in hyperbolic metamaterials for polarization-controlled routing of subwavelength modes *Nat. Commun.* **5** 3226
- [96] Lee Y U and Wu J W 2015 Control of optical spin Hall shift in phase-discontinuity metasurface by weak value measurement post-selection *Sci. Rep.* **5** 13900
- [97] Wang B *et al* 2013 Spin displacements of a Gaussian beam at an air–multilayer-film interface *Phys. Rev. A* **88** 043842
- [98] Zhou X *et al* 2013 Photonic spin Hall effect in topological insulators *Phys. Rev. A* **88** 053840
- [99] Luo H, Wen S, Shu W and Fan D 2010 Spin Hall effect of light in photon tunneling *Phys. Rev. A* **82** 043825
- [100] Zhou X, Ling X, Zhang Z, Luo H and Wen S 2014 Observation of spin Hall effect in photon tunneling via weak measurements *Sci. Rep.* **4** 7388
- [101] Qin Y *et al* 2011 Observation of the in-plane spin separation of light *Opt. Exp.* **19** 9636–45
- [102] Pan M *et al* 2013 Impact of in-plane spread of wave vectors on spin Hall effect of light around Brewster’s angle *Appl. Phys. Lett.* **103** 071106
- [103] Qiu X *et al* 2015 Incident-polarization-sensitive and large in-plane-photonic-spin-splitting at the Brewster angle *Opt. Lett.* **40** 1018–21
- [104] Ren J *et al* 2012 Spin Hall effect of light reflected from a magnetic thin film *Appl. Phys. Lett.* **101** 171103
- [105] Aiello A and Woerdman J P 2008 Role of beam propagation in Goos–Hänchen and Imbert–Fedorov shifts *Opt. Lett.* **33** 1437–9
- [106] Merano M, Aiello A, Van Exter M P and Woerdman J P 2009 Observing angular deviations in the specular reflection of a light beam *Nat. Photon.* **3** 337–40
- [107] Resch K J 2008 Amplifying a tiny optical effect *Science* **319** 733–4
- [108] Fedoseyev V G 2001 Spin-independent transverse shift of the centre of gravity of a reflected and of a refracted light beam *Opt. Commun.* **193** 9–18
- [109] Bliokh K Y 2006 Geometrical optics of beams with vortices: Berry phase and orbital angular momentum Hall effect *Phys. Rev. Lett.* **97** 043901
- [110] Bliokh K Y and Desyatnikov A S 2009 Spin and orbital Hall effects for diffracting optical beams in gradient-index media *Phys. Rev. A* **79** 011807

- [111] Fedoseyev V G 2009 Conservation laws and angular transverse shifts of the reflected and transmitted light beams *Opt. Commun.* **282** 1247–51
- [112] Merano M, Hermosa N and Woerdman J P 2010 How orbital angular momentum affects beam shifts in optical reflection *Phys. Rev. A* **82** 023817
- [113] Xiao Z, Luo H and Wen S 2012 Goos–Hänchen and Imbert–Fedorov shifts of vortex beams at air-left-handed-material interfaces *Phys. Rev. A* **85** 053822
- [114] Okuda H and Sasada H 2006 Huge transverse deformation in nonspecular reflection of a light beam possessing orbital angular momentum near critical incidence *Opt. Exp.* **14** 8393–402
- [115] Okuda H and Sasada H 2008 Significant deformations and propagation variations of Laguerre–Gaussian beams reflected and transmitted at a dielectric interface *J. Opt. Soc. Am. A* **25** 881–90
- [116] Dasgupta R and Gupta P K 2006 Experimental observation of spin-independent transverse shift of the centre of gravity of a reflected Laguerre–Gaussian light beam *Opt. Commun.* **257** 91–6
- [117] Zhang J *et al* 2014 Orbit–orbit interaction and photonic orbital Hall effect in reflection of a light beam *Chin. Phys. B* **23** 064215
- [118] Aharonov Y, Albert D and Vaidman L 1988 How the result of a measurement of a component of the spin of a spin-1/2 particle can turn out to be 100 *Phys. Rev. Lett.* **60** 1351–4
- [119] Lundeen J S, Sutherland B, Patel A, Stewart C and Bamber C 2011 Direct measurement of the quantum wavefunction *Nature* **474** 188–91
- [120] Kocsis S *et al* 2011 Observing the average trajectories of single photons in a two-slit interferometer *Science* **332** 1170–3
- [121] Kofman A G, Ashhab S and Nori F 2012 Nonperturbative theory of weak pre- and post-selected measurements *Phys. Rep.* **520** 43–133
- [122] Bliokh K Y, Bekshaev A Y, Kofman A G and Nori F 2013 Photon trajectories, anomalous velocities and weak measurements: a classical interpretation *New J. Phys.* **15** 073022
- [123] Dressel J, Malik M, Miatto F M, Jordan A N and Boyd R W 2014 Colloquium: understanding quantum weak values: basics and applications *Rev. Mod. Phys.* **86** 307–16
- [124] Dressel J, Bliokh K Y and Nori F 2014 Classical field approach to quantum weak measurements *Phys. Rev. Lett.* **112** 110407
- [125] Qin Y, Li Y, He H and Gong Q 2009 Measurement of spin Hall effect of reflected light *Opt. Lett.* **34** 2551–3
- [126] Jayaswal G, Mistura G and Merano M 2013 Weak measurement of the Goos–Hänchen shift *Opt. Lett.* **38** 1232–4
- [127] Santana O J, Carvalho S A, De Leo S and de Araujo L E 2016 Weak measurement of the composite Goos–Hänchen shift in the critical region *Opt. Lett.* **41** 3884–7
- [128] Geszti T 2010 Postselected weak measurement beyond the weak value *Phys. Rev. A* **81** 044102
- [129] Wu S and Li Y 2011 Weak measurements beyond the Aharonov–Albert–Vaidman formalism *Phys. Rev. A* **83** 052106
- [130] Zhou X, Li X, Luo H and Wen S 2014 Optimal preselection and postselection in weak measurements for observing photonic spin Hall effect *Appl. Phys. Lett.* **104** 051130
- [131] Chen S, Zhou X, Mi C, Luo H and Wen S 2015 Modified weak measurements for detecting photonic spin Hall effect *Phys. Rev. A* **91** 062105
- [132] Gorodetski Y *et al* 2012 Weak measurements of light chirality with a plasmonic slit *Phys. Rev. Lett.* **109** 013901
- [133] Dennis M R and Götte J B 2012 The analogy between optical beam shifts and quantum weak measurements *New J. Phys.* **14** 073013
- [134] Götte J B and Dennis M R 2012 Generalized shifts and weak values for polarization components of reflected light beams *New J. Phys.* **14** 073016
- [135] Aiello A, Lindlein N, Marquardt C and Leuchs G 2009 Transverse angular momentum and geometric spin Hall effect of light *Phys. Rev. Lett.* **103** 100401
- [136] Korger J *et al* 2014 Observation of the geometric spin Hall effect of light *Phys. Rev. Lett.* **112** 113902
- [137] Bekshaev A Y 2009 Oblique section of a paraxial light beam: criteria for azimuthal energy flow and orbital angular momentum *J. Opt. A* **11** 094003
- [138] Korger J *et al* 2011 Geometric spin Hall effect of light at polarizing interfaces *Appl. Phys. B* **102** 427–32
- [139] Kong L, Qian S, Ren Z, Wang X and Wang H 2012 Effects of orbital angular momentum on the geometric spin Hall effect of light *Phys. Rev. A* **85** 035804
- [140] Neugebauer M *et al* 2014 Geometric spin Hall effect of light in tightly focused polarization-tailored light beams *Phys. Rev. A* **89** 013840
- [141] Neugebauer M, Grosche S, Rothau S, Leuchs G and Banzer P 2016 Lateral spin transport in paraxial beams of light *Opt. Lett.* **41** 3499–502
- [142] Bliokh K Y and Nori F 2012 Relativistic Hall effect *Phys. Rev. Lett.* **108** 120403
- [143] Bliokh K Y and Nori F 2012 Spatiotemporal vortex beams and angular momentum *Phys. Rev. A* **86** 033824
- [144] Bliokh K Y, Izdebskaya Y V and Nori F 2013 Transverse relativistic effects in paraxial wave interference *J. Opt.* **15** 044003
- [145] Huang L *et al* 2013 Helicity dependent directional surface plasmon polariton excitation using a metasurface with interfacial phase discontinuity *Light: Sci. Appl.* **2** e70
- [146] High A A *et al* 2015 Visible-frequency hyperbolic metasurface *Nature* **522** 192–6
- [147] Ding X *et al* 2015 Ultrathin Pancharatnam–Berry metasurface with maximal cross-polarization efficiency *Adv. Mater.* **27** 1195–200
- [148] Wang S *et al* 2015 Spin-selected focusing and imaging based on metasurface lens *Opt. Exp.* **23** 26434–41
- [149] Luo W *et al* 2015 Photonic spin Hall effect with nearly 100% efficiency *Adv. Opt. Mater.* **3** 1102–08
- [150] Shaltout A, Liu J, Kildishev A and Shalaev V 2015 Photonic spin Hall effect in gap-plasmon metasurfaces for on-chip chiroptical spectroscopy *Optica* **2** 860
- [151] Lee Y U *et al* 2016 Spin- and orbital-Hall effect in cyclic group symmetric metasurface (arXiv:1607.04806)
- [152] Kildishev A V, Boltasseva A and Shalaev V M 2013 Planar photonics with metasurfaces *Science* **339** 1232009
- [153] Yu N and Capasso F 2014 Flat optics with designer metasurfaces *Nat. Mater.* **13** 139–50
- [154] Meinzer N, Barnes W L and Hooper I R 2014 Plasmonic meta-atoms and metasurfaces *Nat. Photon.* **8** 889–98
- [155] Zhao Y, Liu X and Alù A 2014 Recent advances on optical metasurfaces *J. Opt.* **16** 123001
- [156] Lin D, Fan P, Hasman E and Brongersma M L 2014 Dielectric gradient metasurface optical elements *Science* **345** 298–302
- [157] Shaltout A M, Kildishev A V and Shalaev V M 2016 Evolution of photonic metasurfaces: from static to dynamic *J. Opt. Soc. Am. B* **33** 501–10
- [158] Bhandari R 1995 Phase jumps in QHQ phase shifter—some consequences *Phys. Lett. A* **204** 188–92
- [159] Shu W *et al* 2016 Radial spin Hall effect of light *Phys. Rev. A* **93** 013839
- [160] Liu S *et al* 2016 Longitudinal spin separation of light and its performance in three-dimensionally controllable spin-dependent focal shift *Sci. Rep.* **6** 20774
- [161] Kang M *et al* 2012 Spatial splitting of spin states in subwavelength metallic microstructures via partial conversion of spin-to-orbital angular momentum *Phys. Rev. A* **85** 035801
- [162] Ling X, Zhou X, Luo H and Wen S 2012 Steering far-field spin-dependent splitting of light by inhomogeneous anisotropic media *Phys. Rev. A* **86** 053824

- [163] Li G *et al* 2013 Spin-enabled plasmonic metasurfaces for manipulating orbital angular momentum of light *Nano Lett.* **13** 4148–51
- [164] Ling X, Zhou X, Shu W, Luo H and Wen S 2014 Realization of tunable photonic spin Hall effect by tailoring the Pancharatnam–Berry phase *Sci. Rep.* **4** 5557
- [165] Rashba E I 1960 Properties of semiconductors with an extremum loop. 1. Cyclotron and combinational resonance in a magnetic field perpendicular to the plane of the loop *Sov. Phys. Solid State* **2** 1109–22
- [166] Dahan N, Gorodetski Y, Frischwasser K, Kleiner V and Hasman E 2010 Geometric Doppler effect: spin-split dispersion of thermal radiation *Phys. Rev. Lett.* **105** 136402
- [167] Frischwasser K, Yulevich I, Kleiner V and Hasman E 2011 Rashba-like spin degeneracy breaking in coupled thermal antenna lattices *Opt. Exp.* **19** 23475–82
- [168] Shitrit N, Maayani S, Veksler D, Kleiner V and Hasman E 2013 Rashba-type plasmonic metasurface *Opt. Lett.* **38** 4358–61
- [169] Shitrit N, Yulevich I, Kleiner V and Hasman E 2013 Spin-controlled plasmonics via optical Rashba effect *Appl. Phys. Lett.* **103** 211114
- [170] Gorodetski Y, Shitrit N, Bretner I, Kleiner V and Hasman E 2009 Observation of optical spin symmetry breaking in nanoapertures *Nano Lett.* **9** 3016–9
- [171] Kang M *et al* 2011 Optical spin-dependent angular shift in structured metamaterials *Opt. Lett.* **36** 3942–4
- [172] Liu Y *et al* 2015 Photonic spin Hall effect in dielectric metasurfaces with rotational symmetry breaking *Opt. Lett.* **40** 756–9
- [173] Zhan Q 2009 Cylindrical vector beams: from mathematical concepts to applications *Adv. Opt. Photonics* **1** 1–57
- [174] Wang X *et al* 2011 Unveiling locally linearly polarized vector fields with broken axial symmetry *Phys. Rev. A* **83** 063813
- [175] Zhang Y, Li P, Liu S and Zhao J 2015 Unveiling the photonic spin Hall effect of freely propagating fan-shaped cylindrical vector vortex beams *Opt. Lett.* **40** 4444–7
- [176] Holleccek A, Aiello A, Gabriel C, Marquardt C and Leuchs G 2011 Classical and quantum properties of cylindrically polarized states of light *Opt. Exp.* **19** 9714–36
- [177] Milione G, Sztul H I, Nolan D A and Alfano R R 2011 Higher-order Poincaré sphere, Stokes parameters, and the angular momentum of light *Phys. Rev. Lett.* **107** 053601
- [178] Padgett M J and Allen A 1995 The Poynting vector in Laguerre–Gaussian laser modes *Opt. Commun.* **121** 36–40
- [179] Arlt J 2003 Handedness and azimuthal energy flow of optical vortex beams *J. Mod. Opt.* **50** 1573–80
- [180] Davis J A and Bentley J B 2005 Azimuthal prism effect with partially blocked vortex-producing lenses *Opt. Lett.* **30** 3204–6
- [181] Bekshaev A Y, Mohammed K A and Kurka I A 2014 Transverse energy circulation and the edge diffraction of an optical vortex beam *Appl. Opt.* **53** B27–37
- [182] Rozhkov A V, Sboychakov A O, Rakhmanov A L and Nori F 2016 Electronic properties of graphene-based bilayer systems *Phys. Rep.* **648** 1–104
- [183] Gupta A, Chen G, Joshi P, Tadigadapa S and Eklund P C 2006 Raman scattering from high-frequency phonons in supported n-graphene layer films *Nano Lett.* **6** 2667–73
- [184] Ni Z *et al* 2007 Graphene thickness determination using reflection and contrast spectroscopy *Nano Lett.* **7** 2758–63
- [185] Xiao S, Zhong F, Liu H, Zhu S and Li J 2015 Flexible coherent control of plasmonic spin-Hall effect *Nat. Commun.* **6** 8360
- [186] Cardano F and Marrucci L 2015 Spin–orbit photonics *Nat. Photon.* **9** 776–8
- [187] Ke Y *et al* 2016 Optical integration of Pancharatnam–Berry phase lens and dynamical phase lens *Appl. Phys. Lett.* **108** 101102
- [188] Bliokh K Y and Nori F 2012 Transverse spin of a surface polariton *Phys. Rev. A* **85** 061801
- [189] Bliokh K Y, Bekshaev A Y and Nori F 2014 Extraordinary momentum and spin in evanescent waves *Nat. Commun.* **5** 3300
- [190] Aiello A, Banzer P, Neugebauer M and Leuchs G 2015 From transverse angular momentum to photonic wheels *Nat. Photon.* **9** 789–95
- [191] Van Mechelen T and Jacob Z 2016 Universal spin-momentum locking of evanescent waves *Optica* **3** 118–26
- [192] Antognozzi M *et al* 2016 Direct measurements of the extraordinary optical momentum and transverse spin-dependent force using a nano-cantilever *Nat. Phys.* **12** 731–5
- [193] Lee S Y *et al* 2012 Role of magnetic induction currents in nanoslit excitation of surface plasmon polaritons *Phys. Rev. Lett.* **108** 213907
- [194] Rodríguez-Fortuño F J *et al* 2013 Near-field interference for the unidirectional excitation of electromagnetic guided modes *Science* **340** 328–30
- [195] Petersen J, Volz J and Rauschenbeutel A 2014 Chiral nanophotonic waveguide interface based on spin–orbit interaction of light *Science* **346** 67–71
- [196] Mitsch R, Sayrin C, Albrecht B, Schneeweiss P and Rauschenbeutel A 2014 Quantum state-controlled directional spontaneous emission of photons into a nanophotonic waveguide *Nat. Commun.* **5** 5713
- [197] Alizadeh M H and Reinhard B M 2016 Emergence of transverse spin in optical modes of semiconductor nanowires *Opt. Exp.* **24** 8471–9
- [198] Le Feber B, Rotenberg N and Kuipers L 2015 Nanophotonic control of circular dipole emission *Nat. Commun.* **6** 6695
- [199] Söllner I *et al* 2015 Deterministic photon-emitter coupling in chiral photonic circuits *Nat. Nanotechnol.* **10** 775–8
- [200] Lefier Y and Grosjean T 2015 Unidirectional sub-diffraction waveguiding based on optical spin–orbit coupling in subwavelength plasmonic waveguides *Opt. Lett.* **40** 2890–3
- [201] Espinosa-Soria A and Martínez A 2016 Transverse spin and spin–orbit coupling in silicon waveguides *IEEE Photon. Tech. Lett.* **28** 1561–4
- [202] Zeng H, Dai J, Yao W, Xiao D and Cui X 2012 Valley polarization in MoS<sub>2</sub> monolayers by optical pumping *Nat. Nanotechnol.* **7** 490–3
- [203] Mak K F, He K L, Shan J and Heinz T F 2012 Control of valley polarization in monolayer MoS<sub>2</sub> by optical helicity *Nat. Nanotechnol.* **7** 494–8



**Xiaohui Ling** received the B.S. degree in electronic information science from Hengyang Normal University, Hengyang, China, in 2005, and the PhD degree in optics from Hunan University, Changsha, China, in 2012. He was a postdoc with the SZU–NUS Collaborative Innovation Center for Optoelectronic and Technology, Shenzhen University, Shenzhen, China, until 2015. He was also a visiting scholar with the Department of Electrical & Computer Engineering, National University of Singapore, Singapore, in 2015. He is currently an Associate Professor in Hengyang Normal University. His current research interests include optical spin–orbit interaction, spin Hall effect of light, geometric phase and metamaterials/

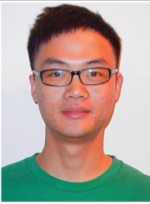
metasurfaces.



**Xinxing Zhou** received the B.S. degree in electronic information science and technology from Hunan Normal University, Changsha, China, in 2010, and the PhD degree in circuits and systems from Hunan University, Changsha, China, in 2015. He is currently an Assistant Professor in Hunan Normal University. His current research interests focus on spin photonics, weak measurements, polarization state manipulation, and metasurfaces.



**Kun Huang** got his PhD degree in optics from University of Science and Technology of China. He is currently a research scientist at Institute of Materials Research and Engineering, A\*STAR, Singapore. His research interests are optics, nanophotonics, and their applications in optical nanofocusing, super-resolution imaging, metasurface holography, orbital angular momentum, and the interaction between photons and materials.



**Yachao Liu** received the B.Eng. degree in electronic science and technology from Hunan University, Changsha, China, in 2013. He is currently a PhD student in physics at Hunan University, Changsha, China. His research interests are in photonic spin Hall effect, vector beams, topological phase, metamaterials/metasurfaces, and photonic crystals.



**Cheng-Wei Qiu** received the B.Eng. degree in applied electromagnetics from the University of Science and Technology of China, Hefei, China, in 2003, and the PhD degree in electromagnetic wave theory for complex media from the National University of Singapore (NUS), Singapore, in 2008. He was a Post-Doctoral Fellow with the Physics Department (with a specialization in transformation electromagnetics and metamaterials), Massachusetts Institute of Technology, Cambridge, MA, USA, until 2009. In 2009, he joined NUS, as an Assistant Professor, and was promoted to Associate Professor in January 2017. He also held Visiting Professor positions with the University of Paris-Sud, Paris, France, KAUST, Saudi

Arabia, and Shenzhen University, Shenzhen, China. He has authored over 150 journal peer-reviewed papers and has given three keynote presentations in international conferences. His current research interests include electromagnetic wave theory of transformation optic metamaterials, light–matter interaction, metasurface and nanophotonics. Prof. Qiu was a recipient of the SUMMA Graduate Fellowship in Advanced Electromagnetics in 2005, the IEEE Antennas and Propagation Society Graduate Research Award in 2006, the URSI Young Scientist Award in 2008, the NUS Young Investigator Award in 2011, the MIT TR35 Singapore Award in 2012, the Young Scientist Award of the Singapore National Academy of Science in 2013, and the Faculty Young Research Award of NUS in 2013. He has been a Topical Editor for the Journal of the Optical Society of America B since 2016. He has served as an Editorial Board Member for various journals and, General Chair and TPC Chairman for various conferences.



**Hailu Luo** received the PhD degree in theoretical physics from Nanjing University, Nanjing, China, in 2007. In 2007, he joined Hunan University, as an assistant professor, and was promoted to Associate Professor in 2009. He established the laboratory for spin photonics and is currently the head of the spin photonics group. He has authored over 100 journal peer-reviewed papers on spin photonics. His current research interests include fundamental theory of spin photonics, geometric phases, quantum weak measurements, spin-momentum locking of light, and spin–orbit interaction of light in 2D atomic crystals.



**Shuangchun Wen** received the B.S. degree in physics from Hunan Normal University, Changsha, China, the M.S. degree in physics from Central China Normal University, Wuhan, China, and the PhD degree in optics from the Shanghai Institute of Optics and Fine Mechanics, Chinese Academy of Sciences, Shanghai, China, in 1987, 1994, and 2001, respectively. Since 2002, he has been a Professor with Hunan University, Changsha, China, where he is currently the Head of the Photonics Technology Research Group. He has authored and coauthored more than 200 scientific publications in international indexed journals and conferences. He holds or co-holds more than 20 patents. His research interests include

studies of nonlinear optics, laser technology, photonic devices, and optical communications. He is a member of the Optical Society of America (OSA) and the International Society for Optical Engineering.